Investigation of Graphene as a Powder and in a Resin Coating

by

Nam NGUYEN

THESIS PRESENTED TO ÉCOLE DE TECHNOLOGIE SUPÉRIEURE
IN PARTIAL FULFILLMENT FOR A MASTER DEGREE
WITH THESIS IN CONSTRUCTION ENGINEERING
M.A.Sc.

MONTREAL, JULY 10TH, 2019

ÉCOLE DE TECHNOLOGIE SUPÉRIEURE
UNIVERSITÉ DU QUÉBEC

BOARD OF EXAMINERS

THIS THESIS HAS BEEN EVALUATED

BY THE FOLLOWING BOARD OF EXAMINERS

Mme Claudiane Ouellet Plamondon, Thesis Supervisor
Department of Construction Engineering, École de technologie supérieure

Mr. Ali Motamedi, President of the Board of Examiners
Department of Construction Engineering, École de technologie supérieure

Mr. Éric David, Member of the jury
Department of Mechanical Engineering, École de technologie supérieure

THIS THESIS WAS PRENSENTED AND DEFENDED

IN THE PRESENCE OF A BOARD OF EXAMINERS AND PUBLIC

ON JUNE 10, 2019

AT ÉCOLE DE TECHNOLOGIE SUPÉRIEURE

ACKNOWLEDGMENT

Firstly, I would like to thank my supervisor Professor Claudiane Ouellet Plamondon, Professor Éric David and Dr Phuong Tri-Nguyen for the long-term collaboration and the help with building up my academic career with their patience, their support and guidance of my master thesis. Throughout my entire Masters, I greatly enjoy my research and life in the Claudiane's group.

A special thanks to all my colleagues and technicians: Mr. Xuan Dai Nguyen, Mrs. Khouloud Jhimi, Mrs. Nancy Milena Sacristan Celys, Mr. Anas Himmad, Mr. Victor Brial, Mr. Honoré Kuate Togue, Mr. Michael Di Mare, Mr. Michael Dubois, Mr. Nabil Mazeghrane, and Mr. Radu Romanica, for the help even during my challenging times.

I would like to thank Mrs. Thi Quynh Nga Vu, Mr. Tuan Tran Anh, Mr. Duc Hoang Minh and their family for the guide of my life in Montréal throughout my Masters study just like my family.

This project was made possible thanks to NanoXplore and especially École de technologie supérieure.

Finally, I would like to give my deepest thanks my parents and friends for their endless love and support. Last but not least, massive thanks to my brother Mr. Sang Nguyen and my beloved girl-friend Ms. Tra, who I shared a lot of significant time and their support was invaluable to me.

Étude du graphène sous forme de poudre et dans un revêtement de résine

Nam NGUYEN

RÉSUMÉ

Le graphène est une monocouche à deux dimensions d'atomes de carbone organisée en réseau hexagonal. La feuille de route d'application du graphène montre qu'il s'agit d'une technologie potentiellement perturbatrice. NanoXplore a déjà produit plusieurs générations de graphène et le produit récent est le graphène noir 3X, un graphène de 6 à 10 couches.

Dans la présente étude, en montrant l'incorporation de feuilles de graphène dans une matrice de résine vinylique, nous montrons qu'il est possible de fabriquer des revêtements conducteurs à faible teneur en graphène à haute stabilité thermique. L'analyse thermogravimetrique montre que ces nanocomposites peuvent être utilisés à une temperature inféreure a 300ºC sans décomposition chimique. Les revêtements conducteurs peuvent être obtenus en ajoutant seulement 5% de graphène. La valeur de conductivité la plus élevée est 3,7 x 10^{-2} S/cm avec 20% en poids de G3X, suffisamment élevée pour divers dispositifs électriques. De plus, l'analyse morphologique par SEM et AFM a révélé une distribution uniforme du graphène noir 3X dans la matrice polymere et l'épassseur des feuilles de graphène. Les propriétés mécaniques peuvent être augmentées 1.5 fois en comparant les 5% et 7% en poids de charge de graphène du composite. Cette augmentation est exceptionnelle et rarement mentionnée dans littérature pour ce type de revêtement.

Mots-clés: Nanocomposites, nanomatériaux, résines vinylester, graphène, morphologie, conductivité électrique

Investigation of graphene as a powder and in a resin coating

Nam NGUYEN

ABSTRACT

Graphene is two-dimension monolayers of carbon atoms organized in a hexagonal lattice. The road map of application of graphene shows that this is a potentially disruptive technology. NanoXplore already produced several generations of graphene and the recent product is the Graphene Black 3X, a 6-10 layers' graphene.

In the present investigation, by incorporating black 3X graphene sheets into a vinyl resin matrix, we show that is possible to fabricate low graphene content conductive coatings with high thermal stability. TGA analysis shows that these nanocomposites can be used at a temperature lower than 300ºC without any chemical decomposition. The conductive coatings can be achieved with the addition of only 5 wt.% of graphene. The highest value of conductivity is found to be 3.7×10^{-2} S/cm with 20 wt.% of G3X, sufficiently high for various electrical devices. Furthermore, the morphological analysis by SEM and AFM revealed uniform distribution of black 3X graphene within the polymer matrix and the thickness of graphene sheets. The mechanical properties can be increased 1.5 times comparing 5 wt.% and 7 wt.& loading of the graphene of the composite. This increment is exceptional high and rarely reported in the literature for this kind of coating.

Keywords: Nanocomposites, Nanomaterial, Vinyl ester resins, Graphene, morphology, Electrical conductivity

TABLE OF CONTENTS

Page

LIST OF TABLES

Page

LIST OF FIGURES

Page

LIST OF ABREVIATIONS

3D	Three dimensional
AC	Alternating current
AFM	Atomic force microscopy
BDS	Broadband dielectric spectroscopy
Bio_GOX	Bio-epoxy resin_Graphene OX
CVD	Chemical vapour deposition
DC	Direct current (DC)
DTG	Derivative thermogravimetry
EC	Electrical conductivity
EMI	Electromagnetic interference shielding (EMI)
ESD	Electrostatic discharge
eV	Electron volt
EVA	Ethylene vinyl acetate
fGO	Functionalised graphene oxide
frGO	Functionalised reduced graphene oxide
FTIR	Fourier transform infrared spectroscopy
G3X	Graphene black 3X
GNS	Graphene nanosheets
GO	Graphene oxide
GOX	Graphene black OX
Gr	Graphene
HDPE	High density polyethylene

LDPE	Low density polyethylene
LLDPE	Linear low density polyethylene
MEK	Methyl ethyl ketone
MEKP	Methyl ethyl ketone peroxide
N	Newton
OBRC	Online bioinformatics resources collection
Pa	Pascal
PA	Polyamide
PC	Polycarbonate
PE	Polyethylene
PET	Polyethylene terephthalate
PP	Polypropylene
PS	Polystyrene
PVA	polyvinyl alcohol
PVC	Polyvinyl chloride
PVDF	Polyvinylidene difluoride
rGO	Reduced graphene oxide
SEM	Scanning electron microscope
SERS	Surface-enhanced Raman spectroscopy
TG/DTA	Thermogravimetric/Differential Thermal Analysis
TGA	Thermogravimetric analysis
TrGO	Thermally reduced graphene oxide
UTS	Ultimate tensile strength

UV	Ultraviolet
VE	Vinyl ester
VSR	Vinyl ester resin
VSR+H	Vinyl ester resin and Hardener

LIST OF SYMBOLS

A	Area of the piston surface (cm^2)
F	Correction factor
I	Current (mA)
L	Sample distance (cm)
nm	Nanometre
^oC	Degree Celsius
P	Pressure (Pa)
s	Distance between the probes (mm)
sp^2	Hybridized atoms in sigma and pi bonding
t	Film thickness (mm)
V	Applied voltage (mV)
wt.%	Weight percentage
ρ	Resistivity (Ωcm)
R	Resistance (Ω)
ρ_s	Resistivity of sample (Ωcm)
σ	Electrical conductivity (S/m)

INTRODUCTION

The capability to synthesize nanoparticles of diverse materials, sizes and shapes associated with the ability to assemble them efficiently into complicated structures makes a significant breakthrough in the area of nanoscience (Evanoff Jr. et Chumanov, 2005). The structural characteristics allow nanomaterials to possess a large variety of applications. However, different types of materials owning advanced physicochemical properties were thoroughly investigated to be more dimensionally compatible in the field of nanoscience and technology. The exploration of graphene and graphene-based polymer nanocomposites has consequently become essential in the field of nanoscience particularly and in the era of science and technology (Stankovich et al., 2006).

There has been an increasingly positive concern about polymer nanocomposites in the recent years thanks to their improved properties derived from the reinforcement of nanofillers (Kim, Abdala et Macosko, 2010; Potts et al., 2011). In comparison with the conventional micron scale fillers, the properties of the composites are considerably influenced by the dispersion of the nanofilleres inside the polymer matrix (Kuilla et al., 2010). Graphene is a one-atom-thick planar sheet of sp^2-bonded carbon atoms and emerges as a potentially multifunctional nanofiller owning to its range of strengths, namely exceptionally high electrical and thermal conductivities, enormous mechanical properties and affordably-priced manufacture. It is additionally seen as the “thinnest material in the universe” with a great potential for different applications (Dreyer et al., 2010; Si et Samulski, 2008).

NanoXplore is a company located in Montreal and it has expertise on graphene commercial at a low cost, large volume and highly scalable. Graphene is two-dimension monolayers of carbon atoms organized in a hexagonal lattice. The road map of application of graphene shows that this is a potentially disruptive technology. NanoXplore already produced several generations of graphene and the recent product is the Graphene Black 3X, a 6-10 layers’ graphene. The potential applications are various, including heat dissipation, EMI shielding, gas barriers, UV resistance, conductive inks and coatings, battery electrodes, smart

composites, electrostatic discharge (ESD) and anti-static. Graphene may also be used for latest innovative technologies such as production of hydrogen from water (Peng et al., 2018); enhanced surface-enhanced Raman spectroscopy (SERS) (Liu et al., 2018), storage energy (Pei et al., 2018) and fast water transport (Xie et al., 2018).

The current data sheet does not contain information about the basic conductivity of this material. NanoXplore has an important line of activity in graphene that needs more investigations on several aspects including: coating materials and methods, durability, conductivity. Regarding graphene based nanocomposites, NanoXplore has developed strict collaboration and funded to some research groups to prepare smart graphene-polymer nanocomposites: i) conducting polymer from polyethylene (PE)/graphene (Moghimian et al., 2017), ii) EVA/graphene, iii) super thermally conductive PE/graphene nanoplatelets (Hamidinejad et al., 2018), iv) super-high heat dissipation poly (vinyldene fluoride)/graphene nanoplatelets composites to improve electromagnetic shielding (Zhao et al., 2017a).

Vinyl ester resins are thermoset matrices, which are widely applied in the industry of composites (Changwoon Jang, 2012; Liao et al., 2010). It is the esterification of epoxy resin with unsaturated monocarboxylic acid that manufactures the VE resin. The environment which is suitable for the resins requires high corrosion and chemical resistance, water barrier properties, low moisture absorption, low shrinkage and good dimensional stability (Anupama Chaturvedi, 2013; Zhanhu Guo, 2006). Owing a variety of advantages, these resins have been extensively used in number of applications such as matrix material, coating, adhesive, electronic encapsulate, in the marine industry, pipelines and automotives (Guo, 2009; Thostenson et Chou, 2006; Zhang et al., 2014).

Objectives of the Master thesis

The general objective of this project is to prepare and characterize graphene/vinyl ester nanocomposite. The specific objectives are the following:

- Measure the conductivity of graphene powders;
- Investigate the optimal conditions for the preparation of conducting coating from vinyl ester resin by turning processing conditions (graphene content, temperature, hardness content, sample thickness, and mixing time).
- Investigate the electrical, thermal, mechanical properties of as-prepared coatings.

Thesis outline

In the "Literature review", the mechanism, synthesis and applications on composite materials, a brief overview of thermoset resins, vinyl ester resin, graphene and characterization methods have been introduced.

In the following chapter Materials and methods, Chapter 2 explains the experimental process, materials and test methods involved in making and analyzing Vinyl ester resin/graphene black 3X composite materials.

In chapter 3 Results and discussions, the synthesized samples were characterized by scanning electron microscopy (SEM), atomic force microscopy (AFM), thermogravimetric analysis (TGA), tensile strength measurements, broadband dielectric spectroscopy (BDS) and four-point probe test.
Conclusions and recommendations are made for summary and future research.

Appendix 1 shows exploratory results on graphene black 0X and bio-epoxy resin decomposition. These results were not further analyzed because of the low conductivity.

Original contribution

The aim of the present work is to perform facile and low cost mechanical methods to prepare advanced composite materials. Graphene-based vinyl ester resin composites were successfully prepared by incorporating graphene into the matrix with improved electrical

properties, thermal stability, and mechanical strength. Furthermore, results from this thesis provide better understanding on the new graphene materials and their potential applications in the smart composite materials. The improvement of the material properties, particularly on conductivity of materials contributes to reducing the price and increases the performance of the composite materials. The latter has a direct link to the use of energy efficiency and thus sustainable development.

CHAPTER 1

LITERATURE REVIEW

1.1 Introduction

In this section, the structure and applications of materials (plastic, vinyl ester resins, graphene), characterization methods are introduced.

A composite material is composed of at least two distinct materials. It is typically composed of two phases, a non continuous phase, like a particle, which has superior properties and a continuous phase, the matrix. This review of conducting polymer/graphene nanocomposites highlighted their potential applications in the coming years for material science and construction engineering field.

The overall polymer nanocomposites properties are driven by the optimal conditions for the preparation of conducting coating and the properties of the graphene and vinyl ester resins. Graphene-based is undoubtedly considered as an exceptional material which was studied for different properties, such as thermal properties (Shahil et Balandin, 2012), mechanical properties (Al-Saleh et Sundararaj, 2011), electrical properties (Sanjinés et al., 2011), rheological properties (Potts et al., 2011), microwave adsorption (Lee, 2012; Qin et Brosseau, 2012), environmental and toxicological impacts (Singh et al., 2011), tailoring with preparation methods (van Rooyen, Karger-Kocsis et David Kock, 2015), and gas barrier properties (Kim, Abdala et Macosko, 2010). The polymer nanocomposites and graphene have been currently used to widespread applications in electronics (Bkakri et al., 2014), bio-electric sensors (Lian et al., 2015), energy technology (Abdin et al., 2013), lithium batteries (Sun et al., 2014), aerospace (Azeez et al., 2013), and various other fields of nanotechnology (Agnihotri, Chowdhury et De, 2015).

1.2 Materials

The matrix of the composite studied in this master thesis is made of plastic, more specifically a thermoset resin. In this section, the classification of plastic is explained, then the composite polymer and graphene is introduced.

1.2.1 Plastic classification

Plastic plays a crucial role in a large number of industrial fields such as the automobile, aerospace, transport, and communication. Plastic, a general term for a range of synthetic or semi-synthetic polymer, is extensively applied to almost all the industries. The plastic mainly consists of thermoplastics, thermosets and elastomers families.

The term “plastic” is derived from a Greek word “plastikos” which means the act of molding and shaping (Starr, 2002). The reason behind this term is that plastic is soft and flexible, and in the process of manufacturing, it is molded and reshaped into many different structures such as films, fibers, plates, and bottles (Robertson, 2005). In the 21st century, plastics are widely used to replace products made of fabric, wood, metal, glass, etc. as they featured as the optimal materials which are light-weight, chemically and mechanically resilient, easy to form and can accommodate many functional additives (Rhoades, 2008).

Polymers are long chains of molecules and they can be organized into two main types: natural polymer and synthetic polymer (Kutz, 2011). Synthetic polymers are classified as either thermoplastics or cross-linked polymers (JMG Cowie, 2007) as shown in Fig. 1.1. This study will focus on thermoplastics and thermoset polymers, which are a subset of crosslinked polymers.

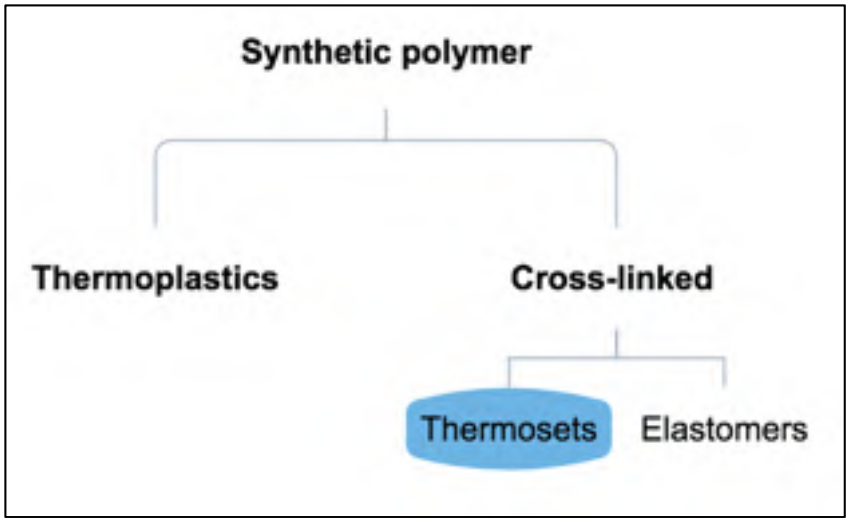

Figure 1.1 The main categories of polymers
Taken from Ouellette et Rawn (2015)

a. Thermoplastics and Thermosets

Thermoplastics are a class of plastics which exhibit a common set of physical properties. Thermoplastics can be formed into stable shapes by heat or pressure (D Hull, 1996). They can also be cast in a liquid form and exhibit no degradation of properties upon resolidification. The most common thermoplastics are polyethylene (PE), polypropylene (PP), polystyrene (PS) and polyvinyl chloride (PVC).

Thermoplastics, which could be reused and cost less than other types of plastic, constitute 75% of the global plastic consumption (Biron, 2018). Having widely been applied to several industries, thermoplastics have increasingly dominated the field of materials worldwide. Polyethylene (and its derivatives HDPE, LDPE, LLDPE) and polypropylene make up more than 60% of the total thermoplastic consumption and are mainly applied to the manufacture of packaging and household products (Beckman, 2018). Constituting 15% of total plastics, PVC has been the third most widely used kind of thermoplastic for manufacturing the materials in the construction industry, for example, pipe, frame or membrane (Beckman, 2018). The final products used in the market are plastic bags, building materials, consumer

products, electronics, and furniture. Figure 1.2 represents the percentage of worldwide utilization of thermoplastics, thermosets and elastomers.

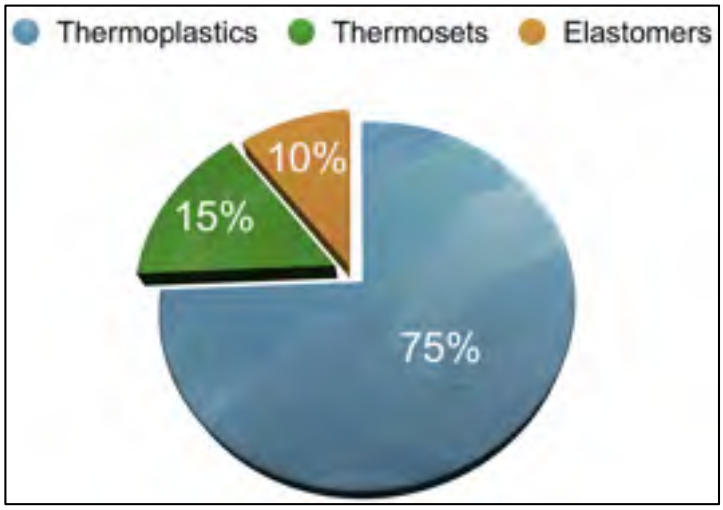

Figure 1.2 The proportion of global use of plastics
Taken from OBRC (2013)

Thermosets are the polymers capable of chemically reacting to form three dimensional (3D) cross-linked structures which cannot, after curing, change their shape by the application of heat (D Hull, 1996). The most well-known thermosets are epoxy, phenolic, polyurethane, and silicone. Thermosets are mainly used in the construction engineering, furniture, logistics, adhesives, electronic devices, inks, and coatings.

b. Plastics by application

Plastics are typically categorized by application. Common plastics are widely used due to their inexpensive source and manufacturing. In particular, polyethylene and polypropylene are the most well known for their applications in consumer products (Maddah, 2016). Engineering plastics, such as those studied in this thesis, are a more specialized class of polymers whose properties surpass those of common plastics and are typically used for the manufacturing of industrial goods (Council, 2005). Specialized plastics are designed for each

use case and are reserved for applications where critical material properties warrant a more expensive material design and manufacturing process (Drobny, 2014).

1.2.2 Thermoset polymer and resins

Due to the 3D cross-linked structure of thermoset polymers, the cannot be converted into the different forms by the application of heat (J-P. Pascault, 2002). Thermoset polymers are obtained by a wide range of cross-linking routes of linear pre-polymers or by the establishment of cross-linked networks from the reaction between two monomers (Saleem et al., 2016). In comparison to thermoplastic materials, thermosets are superior in strength, hardness, and thermal stability (P.E, 2006). To further enhance the quality of thermoset materials, fillers have been incorporated, including clays, carbon nanotubes, and graphene. The most well-known thermosetting polymers in construction materials are epoxies, vinyl ester resin, phenolic, melamine, and urea-formaldehydes, acrylics, urethane and furane. Table 1.1 shows that the thermoset resins are common in the coating industry.

Table 1.1 Summary of construction material applications for thermoset resins
Taken from Pissis (2007)

Thermoset resins	Application
Epoxy	Coating materials- liquid and powder, adhesives, encapsulations, advanced composites, polymer concrete
Vinyl ester	Coatings, adhesives, composites, flooring materials
Phenolic	Advanced composites, composites, rubber reinforcing, polymer concrete, coatings
Melamines and urea-formaldehydes	Molding materials, laminate surfacing materials, foams
Acrylics	Paints, composites, sheeting, casting
Urethane and isocyanurate	Composites, paints, self-skinned moldings
Furane	Tooling

Approximately 90% of the thermosetting resins used in the structural composites are epoxy resins, polyesters, and vinyl esters (Loos, 2015). Table 1.2 gives information on the primary advantages and disadvantages of each type of resin.

Table 1.2 Compare three main of thermoset polymers
Adapted from Loos (2015)

Thermoset polymer	Advantages	Disadvantages
Polyester	• Easy to handle • Cheaper resin than epoxy and vinyl ester	• High styrene emission • High shrinkage after cure
Vinyl ester	• High chemical resistance to the environment • Mechanical properties superior to polyester	• More expensive than polyester • High content of styrene • High shrinkage after cure
Epoxy	• High mechanical and thermal properties • Superior resistance to humidity • Low shrinkage after cure	• More expensive than vinyl ester and polyester resin • Mixture of components is critical

1.2.3 Vinyl ester resin

Vinyl ester resins are unsaturated resins with the high performance which are made from the reaction of different epoxide resins with α-β unsaturated carboxylic acids (Gaur, 2014). The development of vinyl ester resin was to integrate the simplicity and affordable cost of polyesters into thermal and mechanical properties of epoxies. The similarity of vinyl ester resins and polyesters is the molecular structure, and the main difference is placed on location of their reactive groups, which are situated at the end of the chains (Hodgkin, 2001). Vinyl

ester resins are much more long-lasting and sturdy than polyesters because the length of the chains in the former is accessible to absorb impact loads (M.J. Mullins, 2012). The vinyl ester molecule is also characterized by fewer ester groups as shown in Fig. 1.3. These ester groups are likely to be affected by degradation via hydrolysis of water, which demonstrates that vinyl ester is more resilient to water and other chemicals than the polyester (Andreas Kandelbauer, 2013). As a result, it is extensively applied to transmission lines and chemical storages (Loos, 2015).

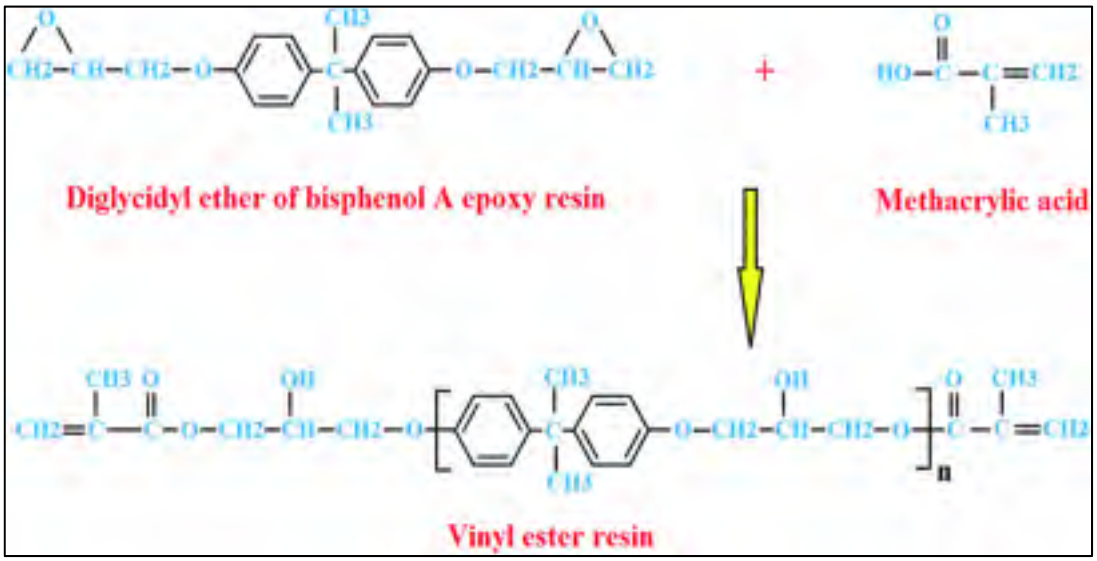

Figure 1.3 Chemical structure composition of vinyl ester resins
Taken from Aghili (2016)

Vinyl ester (VE) based thermosetting polymers are found in a variety of applications thanks to their exceptional mechanical and corrosion resistant properties from their relatively low viscosity of the resin and capability to cure at ambient temperature (Atta, El-Saeed et Farag, 2006; Pauer, 2009; Thostenson, Ziaee et Chou, 2009). The material electrical conductivity is of great importance when it comes to the applications such as aerospace, electronics, adhesives and coatings. The use of a conductive filler, such as graphene, is required to increase the electrical conductivity of the material for those applications (Almajid et al., 2015).

1.2.4 Graphene

Graphene, in its original form, contains a single layer of carbon atoms arranged in a sp^2-bonded aromatic structure as shown in Fig. 1.4 and Fig. 1.5, respectively. It is found as the building block of graphite, where π-stacking of graphene sheets holds the lamellar graphite structure strongly in place with an interlayer spacing of 3.34 Å between the sheets (Hontoria-Lucas et al., 1995). To produce the single layers of graphene, graphite is exfoliated. The sequential cleavage of graphite to graphene employed the use of adhesive tape (Zhu et al., 2010). Geim and Novoselov manufactured the first single-layer graphene sheets (Perreault, Fonseca de Faria et Elimelech, 2015). Their research played an indispensable role in the understanding of the electronic properties of graphene, which was then awarded the Nobel Prize in Physics in 2010 (Geim, 2009; Novoselov, 2007).

Graphene exhibits a large number of exceptional properties which are ideal for some environment-inclined applications. One aspect of graphene which is intensively examined is its electronic properties (Castro Neto et al., 2009; Geim, 2009). Similar to any other nanoscale material, graphene has a high surface area. In theory, graphene exhibits the highest possible surface area, having the theoretical value of 2630 m^2g^{-1}, because each atom of a single-layer graphene sheet participates in two surfaces (Sanchez et al., 2012). The high surface area of graphene allows it to be the perfect material for some processes such as adsorption or surface reactions. Graphene, additionally, is a great support to anchor chemical functionalities or nanomaterials. Graphene-based nanocomposites, therefore, have become the attractive field of research for novel materials (Compton et Nguyen, 2010).

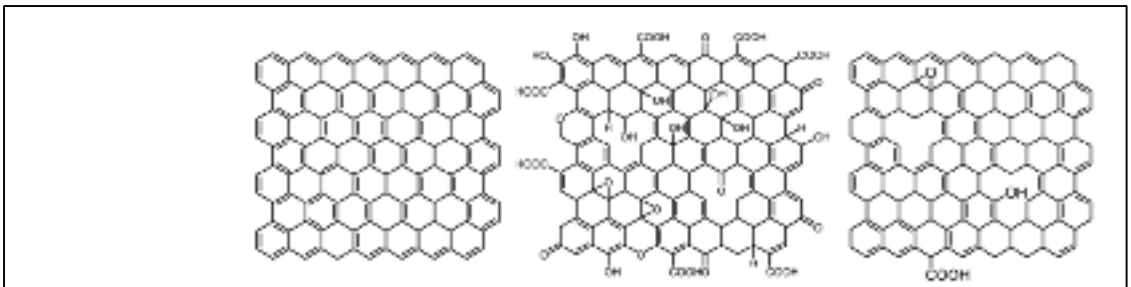

Properties	Graphene	Graphene Oxide	Reduced Graphene Oxide
Synthesis	-Chemical vapor deposition -Thermal decompcsition of SiC -Graphite exfoliation	-Oxidation and exfoliation of graphite	-Reduction of graphene oxide
C:O ratio	No oxygen	2-4	8-246
Young's modulus (TPa)	1	0.2	0.25
Electron mobility ($cm^2 V^{-1} s^{-1}$)	10 000–50 000	insulator	0.05–200
Production cost	High	Low	Low

Figure 1.4 The structure and main properties of graphene-based materials
Adapted from Changgu Lee (2008); Gómez-Navarro, Burghard and Kern, (2008); Park and Ruoff (2009); Sreeprasad and Berry (2013); Suk et al. (2010)

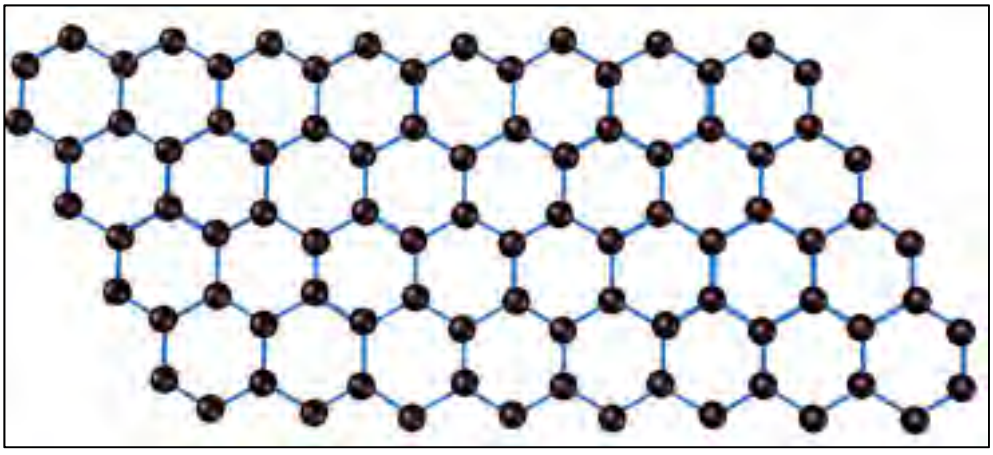

Figure 1.5 The 3D structure of graphene layer

However, some of these characteristics have been achieved only for the high-quality samples (such as mechanically exfoliated graphene) or graphene deposited on special substrates like

hexagonal boron nitride. When developing practical applications, there are three major concerns which need to be addressed: (1) the synthesis of high-quality crystals; (2) to functionalize efficiently functions to each case, and (3) to develop more exceptional applications for graphene (Kuldeep Singh, 2012).

Synthesis

There have been four distinct synthetic methods of graphene, including micro-mechanical exfoliation, chemical vapour deposition (CVD), liquid phase reduction of graphene oxide and epitaxial growth (Kuilla et al., 2010). Of these approaches, direct liquid phase exfoliation is the best to obtain low cost and high throughput material. Hummers and Offeman invented in 1958 what is now regarded as the primary method to create graphene oxide from graphene (Mohan et al., 2016). In this work key techniques were introduced for the production of graphene and its derivatives, which is shown in Fig. 1.6 (Mohan et al., 2018).

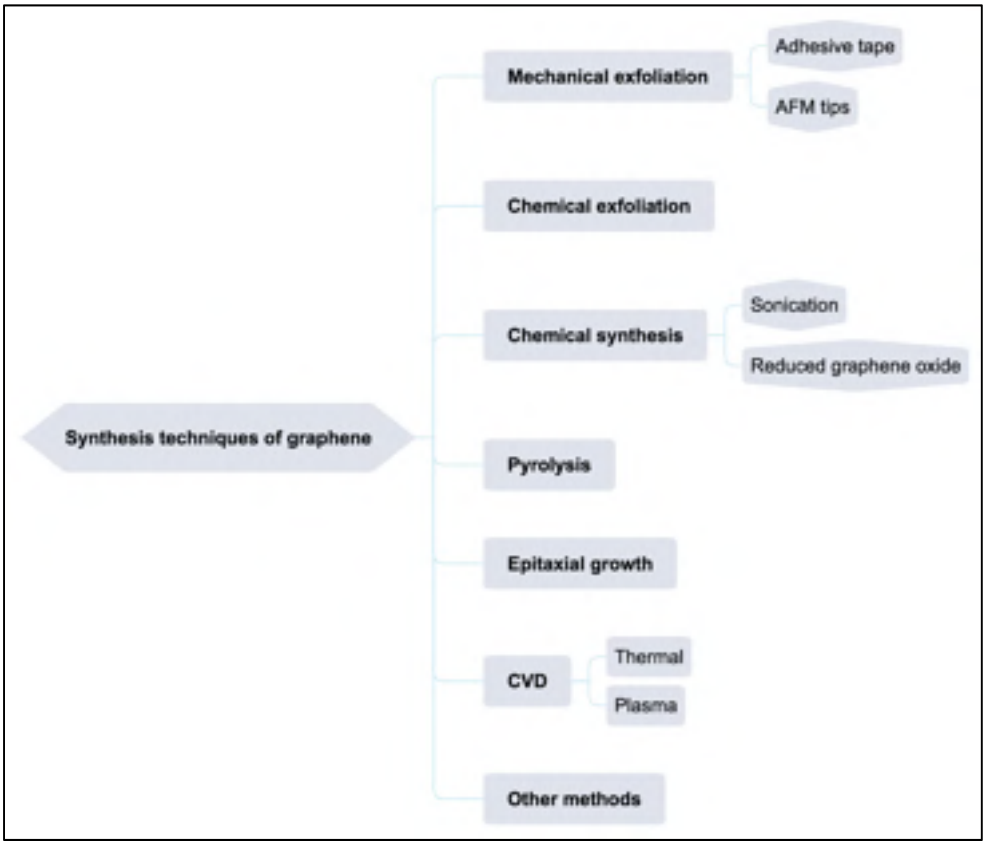

Figure 1.6 The Summary of Synthesis Techniques for Graphene
Adapted from E Malic (2013); Gadipelli and Guo (2015); Georgakilas (2014); Morris JE (2013); Subbiah Alwarappan (2013); Z (2015)

Mechanical properties

Through graphene is only one atom in thickness, it exhibits very high mechanical properties. It is considered the strongest material, with a Young's modulus of E = 1.0 TPa and intrinsic strength of 130 GPa in its pristine, atomically perfect form (Changgu Lee, 2008). Those outstanding mechanical characteristics create the great interest in the application of graphene as a filler to strengthen the mechanical characteristics of softer materials (Potts et al., 2011). Graphene materials possess a large number of outstanding mechanical features, which are also very promising in nano-electromechanical applications. The latest research on the mechanical characteristics of graphene derivatives are shown in Table 1.3.

Table 1.3 Reported Mechanical Properties of Different Graphene Sources

Derivative	Production method	Young's modulus	Reference
Graphene	Mechanical exfoliation	1 TPa	(Frank et al., 2007)
Graphene	Mechanical exfoliation	0.96 TPa	(Faccio et al., 2009)
Graphene	Mechanical exfoliation	0.8 TPa	(Changgu Lee, 2008)
Graphene	Mechanical exfoliation	1.02 TPa	(Kudin K, 2001)
Graphene	Mechanical exfoliation	1.1 TPa	(Van Lier et al., 2000)

Electrical properties

Electrons were observed to possess a high mobility in graphene, reaching 10 000 $cm^2 V^{-1} s^{-1}$ to 50 000 $cm^2 V^{-1} s^{-1}$ at room temperature (Fig. 1.4), with an intrinsic mobility limit of > 200 000 $cm^2 V^{-1} s^{-1}$ (Bolotin et al., 2008; Sreeprasad et Berry, 2013). Without scattering, these charge carriers can be travel sub-micrometer distances and it is known as ballistic transport. Graphene is capable of maintaining current densities up to six order of magnitude higher than copper (Novoselov, 2007). Nevertheless, these electronic characteristics of graphene are only measured under certain conditions, with mechanically exfoliated graphene under vacuum (Bolotin et al., 2008). A number of reasons are attributed to the limitations of the electronic characteristics of graphene, including number of layers, the presence of defects, impurities, functional groups, the size and flatness of the sheet, and the nature of the substrate (Sreeprasad et Berry, 2013; Yang et al., 2010).

A summary of researches on the electrical characteristics of graphene materials is illustrated in Table 1.4. A range of polymer matrices from thermoplastic to thermoset, along with the different weight and volume percentage addition of graphene materials has been examined by various approaches and the results are impressive (Aguilar-Bolados et al., 2016; Mohan et al., 2015; Tang et al., 2012a).

Table 1.4 Literature review on electrical conductivity of different graphene derivatives

Derivative	**Production method**	**Reduction/modifying agent**	**Electrical conductivity ($S.cm^{-1}$)**	**Reference**
Gr	Liquid exfoliation/Vacuum filtration	Hydrazine hydrate	1000	(Wang et al., 2010)
Gr	Liquid exfoliation	Ammonia and hydrazine	5.5	(Chenlu Bao 2012)
rGO	Liquid exfoliation	KOH	60	(Zhang et al., 2012)
GNS	Liquid exfoliation	Hydroquinone		(Wang et al., 2008)
fGO	Liquid exfoliation	Hydrazine and Pyrene groups	~1000	(Su et al., 2009)
TrGO	Liquid exfoliation	Thermal reduction	80	(Worsley et al., 2010)

(Gr: Graphene**,** rGO: reduced graphene oxide, GNS: graphene nanosheets, fGO: unctionalized graphene oxide, TrGO: Thermally reduced graphene oxide)

Thermal properties

Similar to the electrical conductivity, in theory graphene exhibits exceptional thermal properties. However, interfacial interactions and atomic defects can significantly reduce this property. Imperfections in the 2D lattice of graphene create sites for phonon dispersion, dramatically reducing the thermal conductivity. Table 1.5 illustrates literature data on the thermal conductivity values of different graphene materials.

Table 1.5 Literature review on thermal conductivity of different graphene derivatives produced by various methods

Derivative	Production method	Reduction/modifying agent	Thermal conductivity ($KW^{-1}m^{-1}$)	Reference
Graphene	Liquid exfoliation	Thermal reduction	1238	(Kumar et al., 2014)
Single layer graphene	CVD graphene	-	52500	(Hong et al., 2012)
Graphene	-	-	~ 5000	(Prasher, 2010)
Pristine graphene	CVD	-	~ 5000	(Lee et al., 2011)
Graphene	Mechanical exfoliation	-	~ 4840 - 5300	(Pei et Cheng, 2012)

(CVD: Chemical vapour deposition)

1.3 Fabrication and characterization methods

1.3.1 High shear mixer

This work employed a high shear mixer which is also called high shear rotor/stator mixer. The invention of high shear mixer made a breakthrough in the mixing technology, enhancing the processing and manufacturing industries globally. The targeted fields served with this machine are diverse, including food, pharmaceuticals, cosmetics, adhesives and chemicals. Almost all kinds of high shear mixers aim at accomplishing a shared set of objectives, namely homogenization, emulsification, powder wet-out and de-agglomeration. The dominance of the high shear rotor/stator mixer over the conventional mixers originates from the design of workhead, which makes the mixing process highly effective (Zhang, Xu et Li, 2012).

In the first stage, the rotor with the high-speed rotation creates a suction, which forces liquid and solid materials upwards to the workhead. The process moves on with the centrifugal force pushing the materials to the periphery of the workhead at which they are ground between the rotor blades and the stator. Following this step, an intense hydraulic shear happens when the materials are forced out of the stator and return to the mixture. Fresh materials are then pulled into the workhead, which repeats the cycle. The resulting process largely eliminates turbulent material flow and minimizes aeration (Utomo, Baker et Pacek, 2008).

There is a host of advantages a high shear mixer. For many applications, the advanced high shear mixer is manufactured with the capability of reducing mixing times up to 90 percent compared to conventional methods. The specifically-designed workhead allows each machine to perform a variety of functions simultaneously. For instance, in case of oil and water emulsions, a nearly instantaneous stable emulsion can be produced through the high shear mixer in comparison with other available mixers, which can find hard to form the emulsion by a stirrer or an agitator. In another example, thickening agents can be added quickly and form a clear agglomerate-free solution, whereas other conventional agitators require the rather slow and careful act of pouring thickening agents so that agglomerates could be prevented. The mixer can also be used for disintegrating and homogenizing large solids like any types of animal, mineral or synthetic original in a single operation (Kowalski, Cooke et Hall, 2011).

1.3.2 Morphological studies

a. Atomic force microscope (AFM)

An atomic force microscope (AFM) is used to image the micro and nanostructure of materials. AFM is a tool for observing the morphology and measuring the thickness of 3X and OX graphene sheets. In an AFM, a cantilever is attached to a sharp tip is used for scanning the sample surface. When the tip touches the sample surface, the force generated

between the tip and the surface make the cantilever move towards the surface. However, when the cantilever bends closer towards the surface, a controlled repulsive force is exerted on the cantilever to bend away from the surface. An AFM contains 3 crucial devices for different functions. The first instrument is a Z scanner to move the cantilever up and down. In order to move across the sample an XY scanner is employed. The position detector is also added to record the bending of the cantilever. The function of the position sensor is to track a laser beam reflected off the flat top of the cantilever. The direction of the reflected beam is changed if the cantilever is bent. The position detector records those beam changes to map the surface. An AFM records the topographic map of the sample surface by scanning the cantilever over some areas using a feedback loop to control the tip on the surface (Giessibl, 2003).

Unlike other microscopes providing a two-dimensional image of a sample, AFM provides a three-dimensional surface profile. Sample surfaces tested on AFM do not require any special treatments like metal or carbon coatings, which may cause the change or damage for the sample. Most of the AFMs can work efficiently in ambient air or even a liquid environment compared to some microscopes that require a high vacuum environment. AFM is also considered dominant as it provides atomic resolution in ultra-high vacuum and in liquid environments (García et Pérez, 2002).

On the other hand, AFM still has some weak points that need to be fixed. The very first weakness is that AFM is the single size, which can only image a maximum height of 10-20 micrometers and a maximum scanning area of about 150 x 150 micrometers. Another limitation is the scanning speed. AFM requires a large amount of time for a typical scan, which causes the thermal drift in the image. Consequently, AFM is not the proper method for the measurement of accurate distances between topographical features. One more disadvantage is attributed to the hysteresis of the piezoelectric material and cross-talk between the x, y, z piezoelectric actuators, which can affect the AFM images, leading to the fact that the real topographical features can be flattened out. Like any other methods, the

image artifacts can be found by inappropriate tip, poor-quality environment or even by the sample itself (Meyer et Amer, 1988).

b. Scanning electron microscope (SEM)

A scanning electron microscope (SEM) is an accomplished device used for obtaining information on the surface of solid materials through the focused beams of electrons. Thanks to the high-solution and three-dimensional images provided by SEM, a great deal of data about the sample is revealed, including external morphology (texture), chemical composition, crystalline structure and orientation of materials (Joseph I. Goldstein, 2017).

An SEM is comprised of an electron gun, focusing lenses, a high vacuum chamber and a series of electron detectors. The electron gun generates a beam of high-energy electrons down the column and into a series of electromagnetic lenses to focus onto and raster across the sample. This process is conducted on a computer with the support of SEM operator to control magnification and identify the surface area to be scanned. The beam is focused onto the stage, where a solid sample is placed. Sample preparation for the sample is required before being put in the vacuum chamber. All samples require the capability of handling the low pressure inside the vacuum chamber. The acceleration rate of incident electrons, carrying significant amounts of kinetic energy, will determine the interaction between the incident electrons and the surface of the sample. When the interaction happens, energetic electrons are exposed from the surface of the sample. The scattered patterns give information in size, shape, texture and composition of the sample. Several detectors, including backscattered electrons and X-rays, are applied for attracting different types of scattered electrons. Backscatter electrons provide composition data regarding element and compound detection. The data about mineral can be found through X-rays emitted from beneath the sample surface (Reimer, 2013).

SEM is undoubtedly crucial in the fields that require the examination of solid materials. Due to the three-dimensional, topographical images and detailed information from different

detectors, SEM is widely applied for a range of areas, particularly on geological applications. For the most part, almost all SEMs are comparatively easy to operate. The available assistance of computer technology and associated software makes the operation much simpler for operators. The use of this technique is primarily limited by high equipment cost (Goldstein, 2017). In addition to the unit cost, SEMs must be operated in an environment where there is no interference of electricity, magnet and vibration. The requirement for maintenance is also demanding, which involves remaining a stable voltage, currents to electromagnetic coils and circulation of cool water. The preparation of samples can lead to the artifacts, making an adverse impact on the information processing. There is still no absolute way to eliminate or identify the potential artifacts (Goldstein, 2017).

1.3.3 Fourier Transform Infrared (FTIR) spectroscopy

Fourier Transform Infrared (FTIR) is a method used to measure infrared spectrum absorption. FTIR is a mathematical process to turn the data into a visual spectrum. In the infrared spectroscopy, infrared radiation passes through a sample. Some of the infrared radiation is absorbed by the sample and some of it is transmitted. The resulting spectrum shows the molecular absorption and transmission, which forms the molecular fingerprint of the sample. FTIR spectroscopy can be applied to identifying unknown materials, determine the quality or consistency of a sample and the amount of components in a mixture (Smith, 2011).

FTIR spectroscopy offers a number of advantages over other techniques. As all of the frequencies are measured at the same time and spectra are generated in a matter of seconds. The application of FTIR can substantially improve the molecular sensitivity. The noise levels have been observed far lower with the support of the detectors and the higher optical throughput. With regard to the mechanical property, as there exists only one moving part in the machine, the unit is low maintenance. These instruments also use a HeNe laser as an internal wavelength calibration standard which allows them to be self-calibrating (Smith, 2011).

1.3.4 Thermal properties

Thermogravimetric analysis (TGA) is a thermal analysis technique for measuring mass changes of a sample under the condition of raising temperature in a controlled atmosphere. From this measurement, two data sets can be obtained, which are weight loss-time and mass loss-temperature. Thermogravimetric analysis was carried out in a combined system Thermogravimetric/Differential Thermal Analysis (TG/DTA) (JD Menczel, 2009).

This instrument is the combination of a special furnace and a sensitive mass balance. DSC sensor is used to replace the scale pan. In order to limit the impact on the environment, the balance cell is thermostated. The balance beam is then attached to the TGA-DSC sensor. The sample and reference crucibles are set in the center of the furnace. Due to the support of thermal buoyancy and the purge gas flow, the horizontal design of the furnace is able to reduce the possibility of turbulence. Both sides of the furnace are protected with baffles, and the whole volume is purified by a constant flow of gas. The sample can also be purged with a reactive gas flowing through the capillary near the sample crucible. The volatile and gaseous combustion products from the sample, together with the purge gas and reactive gas remove from the furnace through the gas outlet on the left. The process finishes with the connection of analytical devices and the outlet to obtain the gas analysis (Broido, 1969).

A key strength of the TGA technique is its proven dual balance beam to provide drift-free baselines. The efficiency of the dual balance design minimizes the effects of changing purge gases and purge gas flow rates; reducing chimney and convection effects. The system is resilient to external disturbances such as temperature fluctuations and vibrations. High quality results can be obtained even for very low mass weight loss events. With the horizontal balance design of TG/DTA, the gas flow and the weight direction are perpendicular. Consequently, the purge gas flows will cause a limited amount of effect even at rapid purge rates up to 1000 mL/min. Highly condensable or oily volatiles are measured by high purge gas flow since they are purged from the DT-TGA instrument before significant condensation. The act of introducing the corrosive or special purge gases into the furnace

tube helps to minimize the damage to the balance assembly and electronics. Additionally, the maintenance cost and time is reduced by the light weight replaceable parts (Doyle, 1961).

1.3.5 Tensile property

The capacity to minimalize the breakage under tensile stress is one of the most pivotal measured properties of materials for structural applications. In order to quantify this property, the maximum force per unit area (MPa or psi) is measured, known as the ultimate tensile strength or tensile strength at break. The speed at which the sample is pulled apart in the test can be varied between 0.2 and 20 inches per minute and this will have an influence on the results. For the test, composite samples are either manufactured from the stock shapes or injection molded. The machine used to test the tensile strength pulls the samples from both sides and then measures the force required while simultaneously measuring the strain before breaking (Kim et al., 2006).

With this ultimate tensile strength measured, the material characteristics are identified, which allows the materials engineers to forecast whether the materials will react favorably in their designed applications (D Gay, 2007). The data obtained from the tensile test can be also utilized to determine batch quality and consistency in manufacture. However, there are some factors influencing tensile strength such as the effect of additives and impurities, temperature, geometric size and shape of samples, gauge length, orientation and morphology, and surface condition (Zhang et al., 1999).

1.3.6 Electrical properties

a. Four-point probe test

Electrical resistivity is the fundamental material characteristic, which determines the material's opposition to the current flow. The material's resistivity relies on some factors, including the material doping, processing, and environmental factors such as temperature

and humidity. Some characteristics, namely the series resistance, threshold voltage, and capacitance can be influenced by the material's resistivity (Archie, 1942).

A four-point probe is a suitable equipment to quantify the resistivity of semiconductor samples. To measure the substrate resistivity, a current is passed through two outer probes and the voltage is measure through the inner probes (Smits, 1958).

The method of the four-point probe is conducted by contacting four equally spaced probes with a material of unknown resistance. There is a DC current set between the outer two probes, and a voltmeter is employed to test the voltage between the inner two probes. The calculation of the resistivity depends on several factors such as the geometry, the source current and the voltage measurement. To simplify measurements, integrated parameter analyzer accompanied by control software is applied for a variety of material resistances including very high-resistance semiconductor materials (Smits, 1958).

Even though the principle is simple, some experimental problems are still taken into consideration when using a four-point probe. The application of metal into a semiconductor generates a Schottky diode rather than an ohmic contact. The samples with very high or very low resistivity require the modification of the drive current to get the reliable reading. Samples with cut or lapped surfaces are more easily measured than those with polished surfaces (Smits, 1958).

To quantify the resistivity of thin, flat materials including semiconductors or conductive coatings, a four-point collinear probe together with a parameter analyzer has been successfully applied. A few parameter analyzers provide built-in configurable tests, which require the proper calculations. The possibilities of defects such as electronics interference, leakage current, and environmental factors like light and temperature need to be also taken into account to ensure the proper measurements (Schuetze et al., 2004).

The primary advantage of sheet resistance compared to other methods of measuring resistance is that it is independent of the size of the square, which allows the consistent comparison between samples. With the assistance of a four-point probe, it can be easily measured. Another significant strength of using a four-point probe is the contact and wire resistances can be eliminated from the measurement (Schuetze et al., 2004).

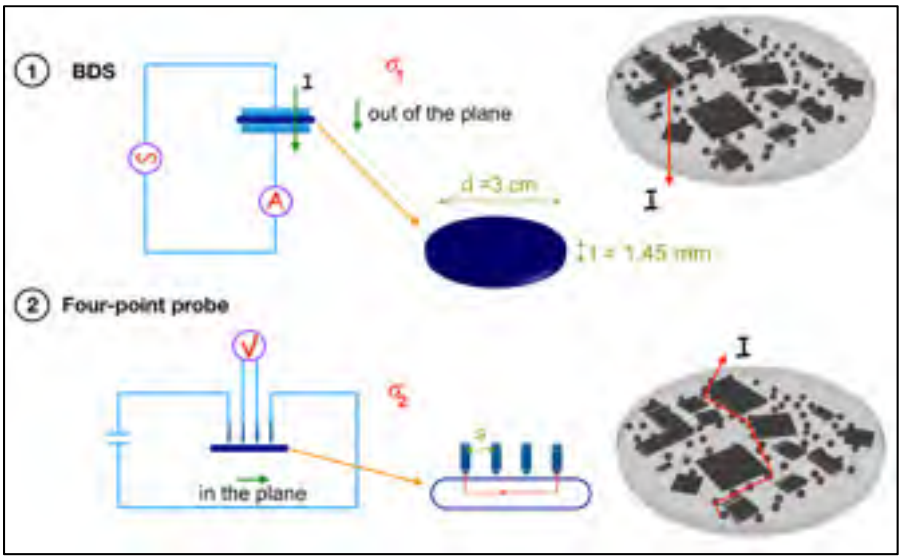

Figure 1.7 Schematic four-point probe and BDS
(dark polygon represents the graphene black, and maroon shows the electron)

b. Broadband dielectric spectroscopy

Broad band dielectric spectroscopy (BDS) is a experimental technique for the purpose of studying the dynamics of polymeric systems. In its current form, BDS can collect data on frequency ranges from 10^{-3} Hz to 10^{9} Hz, extending both limits to lower and higher values (F Kremer, 2012).

Broadband dielectric spectroscopy (BDS) measures the interaction of electromagnetic waves with the frequency range from 10^{-6} Hz to 10^{12} Hz. The substantially wide frequency range provides the study of both molecular fluctuations and collective phenomena, charge and

polarization effects and the dielectric properties of different materials in both liquid and solid form. The versatility of BDS has made it the primary technique in the multidisciplinary design, characterization and application of materials in various fields from nanotechnology to biology (F Kremer, 2012).

BDS quantifies the dielectric permittivity as a function of frequency and temperature. It can also be used to non-conducting materials. The frequency ranges from 10^{-6} Hz to 10^{12} Hz. BDS is sensitive to dipolar species and localized charges, and it determines their strength, their kinetics and their interactions. Dielectric spectroscopy, therefore, is an influential device for measuring electrical properties of non-conducting and semiconducting materials (Kremer, 2002).

Dielectric spectroscopy is based on the interaction of an external electric field with the electric dipole moment and charges of the medium (Stannarius, Kremer et Arndt, 1995). The information on dielectric spectroscopy can be analyzed through a wide range of ways: (i) in terms of dielectric permittivity, (ii) in terms of AC conductivity, (iii) in terms of electric modulus, and (iv) in terms of complex impedance. Those four methods can be applied to identity and analyze the recorded electrical characteristics. In some circumstances, however, a certain method could be more impactful to extract data. The dielectric data, therefore, should be measured in more than one way, especially in the case of the examination of a complicated material as in a nanocomposite.

Due to the high sensitivity with decreasing domain size and wide dynamic range, dielectric spectroscopy has been beneficial in the research of polymer dynamics and in confining geometries. The dielectric characteristics of graphene (dielectric constant, dielectric permittivity, etc.) including polymer nanocomposites are remarkably impacted by the aspect ratio of the graphene and its interfacial adhesion with the polymer matrix (Petzelt et al., 2013).

1.4 Review of the measured properties of polymer composites with graphene

In this section, a thorough investigation of preparing graphene-based polymer composites, including melt blending, solution blending or in-situ polymerisation methods was made. The electrical, thermal and mechanical characteristics are shown to incorporate more effectively with graphene-based filler materials. A list of different graphene based composites and their ultimate tensile strength (UTS) are given in Table 1.6. Electrical conductivities, thermal conductivities of different graphene reinforced polymer composites are given in Table 1.7 and Table 1.8, respectively.

Table 1.6 Literature review on different nanocomposites showing the tensile with respective fabrication methods

Nanocomposites	Filler loading	Fabrication method	UTS (MPa)	Reference
PS/Graphene	1 wt.%	Solution casting	42.5	(Fang et al., 2009)
PP/Graphene	10 wt.%	Melt blending	24	(Song et al., 2011)
PVDF/Graphene	5 wt.%	Solution casting	100	(Layek et al., 2010)
PVA/Graphene	2 wt.%	Solution casting	42	(Wang et al., 2011)
PVA/Graphene	0.7 wt.%	In-Situ	85	(Liang et al., 2009)

(PS: Polystyrene, PP: Polypropylene, PVDF: Polyvinylidene difluoride, PVA: Polyvinyl alcohol)

Table 1.7 Literature review on electrical conductivity values of different polymer graphene composites

Nanocomposites	**Filler loading**	**Fabrication method**	**Electrical conductivity (S.cm-1)**	**Reference**
Polystyrene/Graphene	5 vol.%	Solution casting	1	(Wu et al., 2013)
PET/Graphene	3 vol.%	Melt blending	0.1	(Zhang et al., 2010)
Polyurethane/Graphene	0.015, 0.02, 0.025 vol.%	Melt blending/Solution casting/In-Situ	0.0001	(Kim, Miura et Macosko, 2010)
Polyester/Graphene	1.5 vol.%	Solution casting	1	(Tang et al., 2012b)
EVA/Graphene	15 wt.%	Melt blending/Solution casting	$1x\ 10^{-7}$	(Azizi et al., 2018)

(PET: Polyethylene terephthalate, EVA: Ethylene vinyl acetate)

Table 1.8 Literature review on polymer graphene nanocomposites showing their respective thermal conductivity

Nanocomposites	Filler loading	Fabrication method	Thermal conductivity (WK-1m-1)	Reference
Epoxy/Graphene	4 wt.%	Mechanical stirring and Ultrasonication	1.6	(Teng et al., 2011)
Polyester/Graphene	1.5 vol.%	Solution casting	0.55	(Tang et al., 2012b)
Polypropylene/Graphene	2 vol.%	Melt blending	0.4	(Song et al., 2011)
Epoxy/Graphene/Silver hybrid	5 wt.%	High-shear mixing/Ultrasonication/In-Situ	10	(Goyal et Balandin, 2012)
PVDF/Graphene	10 wt.%	In-Situ	0.58	(Yu et al., 2011)

(PVDF: Polyvinylidene difluoride)

1.5 Application of vinyl ester resin and graphene in coating

In this thesis, the physical properties and synthesis route for a novel vinyl ester resin and graphene nanocomposite material are explained. As previously state, vinyl ester resin is among the class of thermoset polymers which, despite their more complicated forming requirements and low recyclability, see use in a variety of fields. This is primarily due to their increased mechanical properties compared to thermoplastic polymer alternatives. The interest in adding graphene as a filler is twofold: to further improve the mechanical properties of the resin to appeal to existing markets, and to develop new applications through the addition of a new property to the composite, electrical conductivity.

Polymers which exhibit some degree of electrical conductivity are already common in multiple industries. They are used as coatings and additives in a variety of applications,

including integrated de-icing and security coatings for vehicle glass (Mcmaster, 1942) and antistatic coatings for textiles (Gregory et al, 1991). The proposed vinyl ester resin – graphene nanocomposite described herein offers a further alternative in the range of electrically conducive materials for coatings which offers advantages in mechanical stability compared to conventional technology. This material is applicable to many of the same fields as conventional conductive polymers, such as electrical grounding coatings for equipment and factory floors and to electromagnetic shielding applications such as for electrical devices to reduce reception and transmittance of radio interference (Williams et al, 2017).

CHAPTER 2

MATERIALS AND METHODS

2.1 Introduction

This chapter describes the experimental materials, procedures and test methods used through the thesis. Scheme in Fig. 2.1 shows a summary of the work in this master thesis. During the experimental process, the fabrication and tests were carried out on two types of thermoset resin: vinyl ester resin and bio-epoxy resin. The coating with vinyl ester resin was made with graphene 3X and the coating with bio-epoxy with graphene OX. Although graphene black OX exhibits higher electrical conductivity in pure state than graphene black 3X, a very low electrical conductivity in the bio-epoxy composites were measured due to the poor compatibility with the bio-resin matrix as shown with electron imaging. Therefore, the main focus of the thesis is on the experiments and results of vinyl ester resin/graphene black 3X composite materials. The content of bio-epoxy/graphene black OX is included in the section Appendix I as complementary measurements.

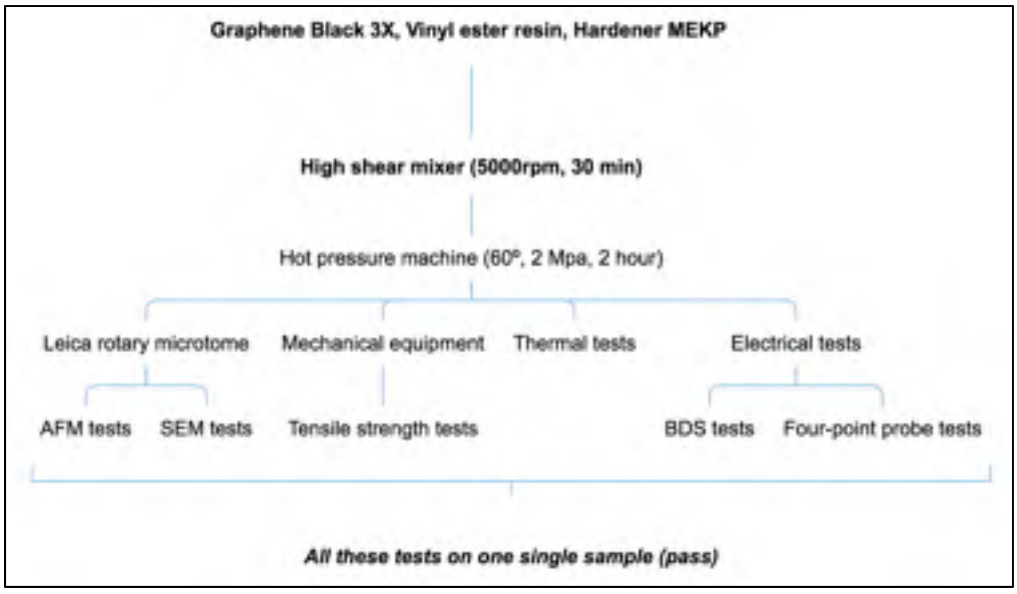

Figure 2.1 The overview of the experimental procedure

2.2 Materials

The constituents of the composites synthesized are vinyl ester resin, methyl ethyl ketone peroxide (MEKP) and graphene black 3X.

2.2.1 Vinyl ester resin

Vipel F010-TBN is a mixture of epoxy-based vinyl ester resin and bisphenol A as a high corrosion resistant additive and fire retardant (molecular weight: ~10,000 to 15,000). The material was supplied by AOC, LLC (USA). The designation codes and characteristics of the vinyl ester resins are shown in Table 2.1.

Table 2.1 Characteristics of the vinyl ester resin

Designation code	**Vipel F010-TBN segment**		**Melting point (ºC)**	**Boiling point**	**Specific Gravity (g/cm^3)**
	Molecular weight	**Content (wt.%)**			
F010-TBN-28	10,000 to 15,000	28	-23.8 F/-30.6 ºC	293 F/145 ºC	1.03

2.2.2 Hardener

As recommended by the manufacturers, the curing of the resin employed a catalyst of methyl ethyl ketone peroxide (MEKP) or Luperox DDM-9 as shown in Fig. 2.2. The use of methyl ethyl ketone (MEK) as a dissolution enables the graphene to disperse in the resin.

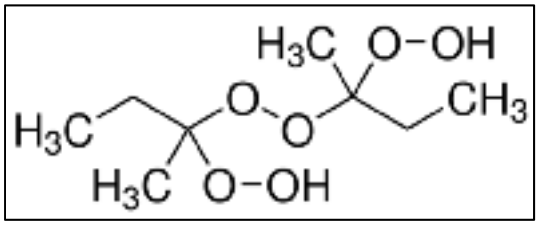

Figure 2.2 Chemical structure of MEKP

Methyl ethyl ketone peroxide, which is also called 2-butanone peroxide, is proven to be an intensely oxidizing (caustic) organic peroxide that is used as a room temperature hardening and curing agent for fiberglass-reinforced plastics and unsaturated polyester resins (HCN, 2002; NTP, 1993).

As MEKP is used as a hardening or curing agent, the period of the reaction largely depends on the types of resins which are being cured and on the formulation of the MEKP. The average reactions consist of 1 to 2% MEKP (CI, 1999). The length of the curing time was approximately 40 – 50 minutes with formulations of commercial MEKP. The curing time is defined as the duration until the resin reaches its peak temperature around 177ºC (350ºF), which is not necessarily the end of the reaction (Puckett, 1997).

2.2.3 Graphene

Graphene Black 3X (G3X) was received from NanoXplore (Canada). Through the technical data sheet of NanoXplore, Graphene Black 3X is seen as a practical powder with the typical flake size of 40 μm. Figure 2.3 presents some main applications of graphene such as heat dissipation, EMI shielding, gas barrier, UV resistance, conductive inks and coatings, battery electrodes, ESD and antistatic.

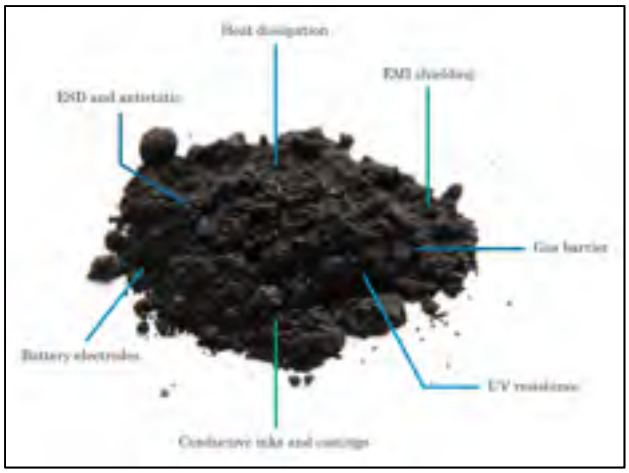

Figure 2.3 The application of graphene black 3X in the industry
(Technical data sheet from NanoXplore)

Physical and chemical properties are illustrated in Table 2.2 and Table 2.3 as following the NanoXplore technical data sheet.

Table 2.2 Physical properties of graphene black 3X

Property	Value
Particle size (laser diffraction)	D_{50}=38 µm
Number of layers	6-10
Bulk density	0.18g/cm^3
Solubility	Insoluble
Moisture (TGA)	<0.7 wt.%
Peak decomposition temperature	750ºC

Table 2.3 The graphene black 3X chemical composition values

Element	Value
Carbon	>91 at.%
Oxygen	<7 at.%
Sulfur	<0.5 at.%
Metal impurities	<2 at.%

2.3 Processing the preparation of vinyl ester resin/graphene composites

Vinyl ester resin/Graphene black 3X composites was prepared at different graphene concentrations by dispersing graphene in vinyl ester resin and subsequently cross-linked the resin using DDM-9. A visualization of the synthesis process is given in Figure 2.4.

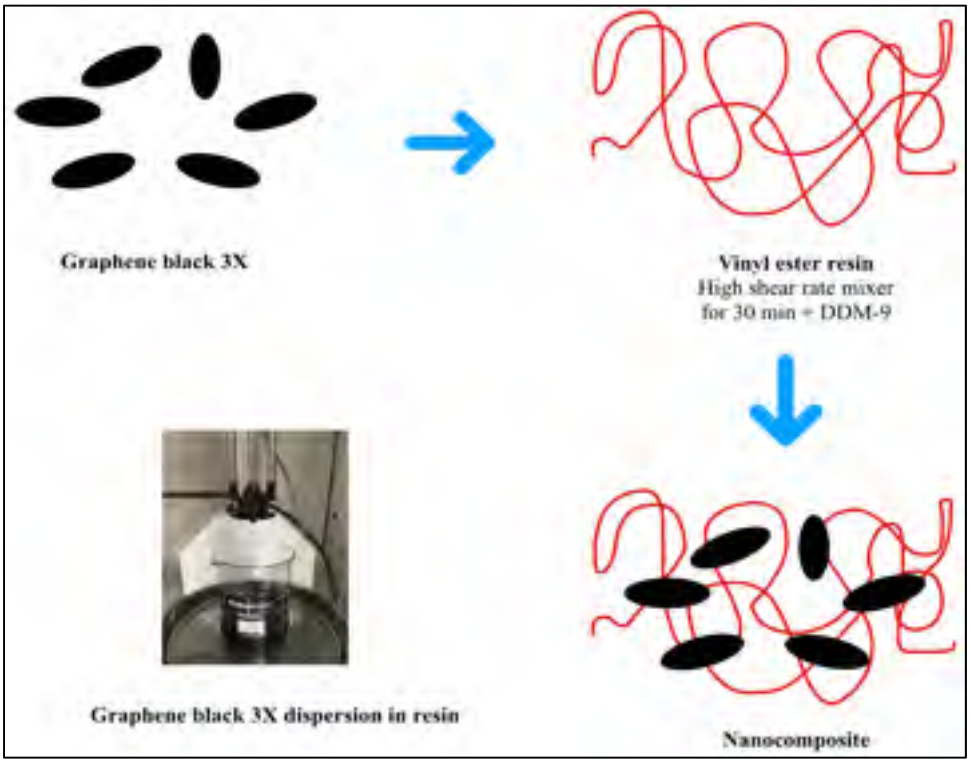

Figure 2.4 Fabrication process of vinyl ester resin/graphene black 3X composite

Vinyl ester resin (VSR)/Graphene black 3X (G3X) composites with different contents: 1, 2.5, 5, 7, 10, 15, 20 wt.% were prepared as follows: a defined graphene content was mixed with 200 grams of vinyl ester resin using high shear rate mixer machine for 30 min with the speed of 5000 rpm. The mixture was then degassed for 30 min under vacuum to remove the air bubbles. Afterwards, 1.5 wt.% of the curing agents Luperox DDM-9 was gradually added into the composite and is molded between two teflon plates. The hot pressure machine is then used to harden the given mixture at 60^{o}C under the pressure of 2 MPa for 2 h. The Table 2.4 shows the volume of materials using in the experiment.

Table 2.4 The proportion of vinyl ester resin and graphene black 3X

The percentage of graphene in the mixture	Vinyl ester resin(g)	Graphene black 3X(g)
VSR-1%G	198	2
VSR-2.5%G	195	5
VSR-5%G	190	10
VSR-7%G	186	14
VSR-10%G	180	20
VSR-15%G	170	30
VSR-20%G	160	40

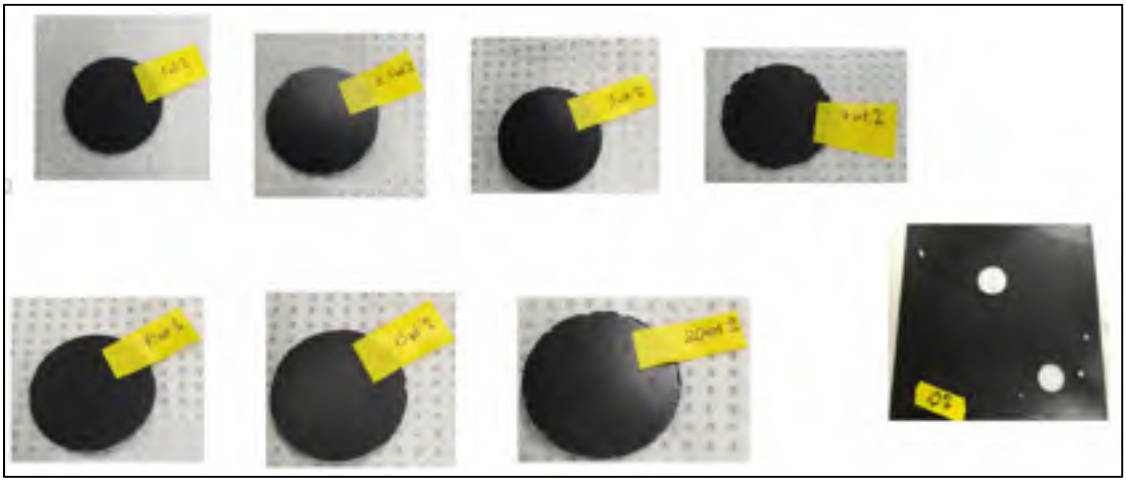

Figure 2.5 The composite samples based on VSR and various G3X contents for electrical conductivity measurements

2.4 Test methods

2.4.1 Electrical properties measurements of graphene black 3X and OX

The electrical conductivity of the 3X and OX graphene powders were measured at room temperature. Every sample was compressed between two brass pistons to form the adjustable (upper) and fixed electrodes (lower) and was put in a hollow cylinder with 27 mm inner diameter. The pressure (P) varied from 0.3 to 200 N by a compressing piston, while the load was measured using Tektronix DMM4040 6-1/2 Digit precision multimeter. A digital vernier

caliper was used to measure the changes in height at each compression step. Conductivity was measured using Tektronix DMM4040 6-1/2 Digit precision multimeter following resistivity and pressure. Ohmic conductivity was measured using following formula :

$$\sigma = \frac{L}{R.A} \tag{2.1}$$

Where σ is electrical conductivity, L is the sample distance, A is the area of the piston surface, and R is resistivity.

2.4.2 Scanning electron microscopy

The SEM technique was used for investigating the surface characteristics of vinyl ester resin and vinyl ester resin/graphene black 3X composites. SEM was accompanied by a Hitachi, Su-8230, FE-SEM microscope with a secondary electron detector using an accelerating voltage of 5kV. In preparation for the analysis, the surface morphology of the samples was covered by platinum using a sputter coater and turbo evaporator Q150T S (Guelph, Canada). This device consists of a turbomolecular pump, to create a vacuum of 5 x 10^{-5} mbar for the sputtering. The specimens' cross-sections were formed by a cryogenic microtome and the thin films were then covered with around 2 nm of sputtered platinum to hinder the charging throughout the SEM analyses. The SEM and turbo-pumped sputter and carbon coater machines are represented in Figure 2.6 and Figure 2.7, respectively.

Figure 2.6 The SEM model Su-8230, FE-SEM equipment in ÉTS laboratory

Figure 2.7 The turbo-pumped sputter machine in ÉTS laboratory

2.4.3 Atomic force microscope

To prepare the samples of polymers for atomic force microscopy analysis, a Leica RM2265 rotary microtome is used to section the samples. A 5 µm thick smooth, uniform section of composite film is formed for each analysis by the Leica RM 2265 as shown in Figure 2.8.

Figure 2.8 Leica RM2265 rotary microsystem
in ÉTS laboratory

An atomic force microscope (AFM) is used to observe the morphology and measure the thickness of the black 3X graphene sheet. The images of AFM from the Université de Montréal laboratory (Figure 2.9) reveals a typical tapping-mode AFM image in which graphene black 3X sheet are directly deposited onto a Si-wafer substrate.

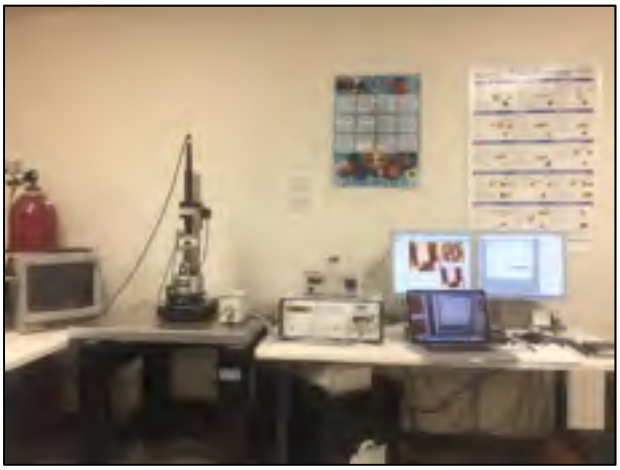

Figure 2.9 AFM images from the Université de Montréal laboratory

2.4.4 Thermogravimetric Analysis

The thermogravimetric analysis (TGA) was conducted to study sample mass changes under rising temperature and controlled atmosphere. From this measurement, two data sets can be obtained, which are weight loss-time and mass loss temperature. The analyses were carried out in a combined system Thermogravimetric/Differential Thermal Analysis (TG/DTA). The melting crucible was composed of platinum, and the analyzed temperature ranges was 200 – 700 °C and with soak at 700 °C for 3 min and a heating rate of 25 °C min^{-1} under a nitrogen flow rate of 50 mL min^{-1}. A sample weight from 10 to 15 mg was selected for each measurement. The main devices for this analysis can be shown in Figure 2.10.

Figure 2.10 Diamond Thermogravimetric/Differential Thermal Analyzer device

2.4.5 Mechanical properties

For measurement of the mechanical properties, dog-bone shaped composite samples were cut such that the distance between the grips was 40 mm, the thickness was1.45 mm and the width was 6 mm as per ASTM E8 (Figure 2.11). The tensile strength measurements were conducted with speed of 2 mm/min at room temperature (Figure 2.12). For each content of fillers, the tensile test was carried out on at least three specimens and the results are averaged.

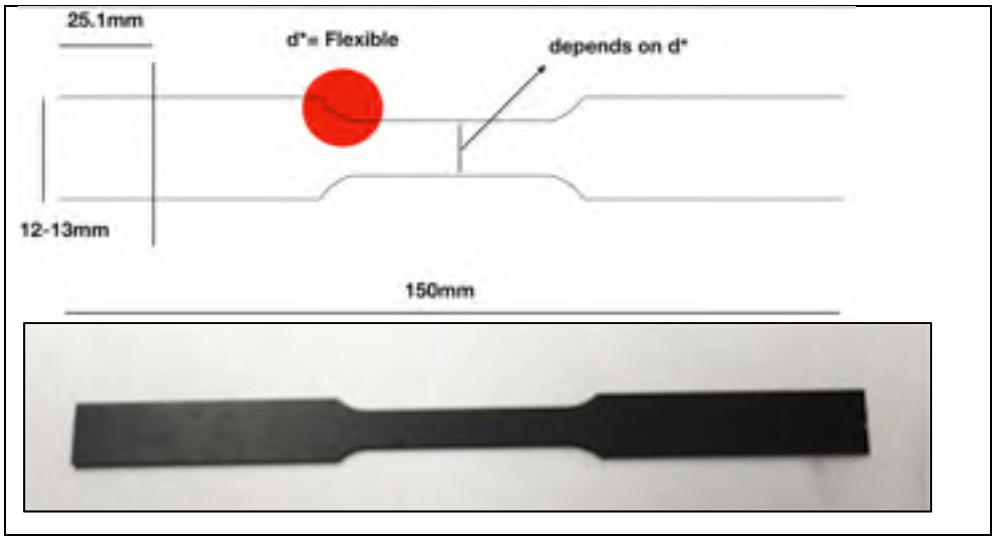

Figure 2.11 Nanocomposite dog-bone specimens for mechanical tests

Figure 2.12 Tensile strength measurement equipment used in this work

2.4.6 Broadband dielectric spectroscopy

The dielectrical properties of composites were measured by a dielectric spectroscopy as a function of frequency (Broadband Dielectric Spectrometer, Novocontrol Technologies). Each sample with a diameter of 3 cmz and average thickness of 1.5 mm was mounted between two brass electrodes for the test (Figure 2.13). Isotherm scans were performed over a frequency from 10^{-2} Hz to 300 kHz under an applied voltage of 3 Vrm/s (corresponding to approximately 2 V/mm).

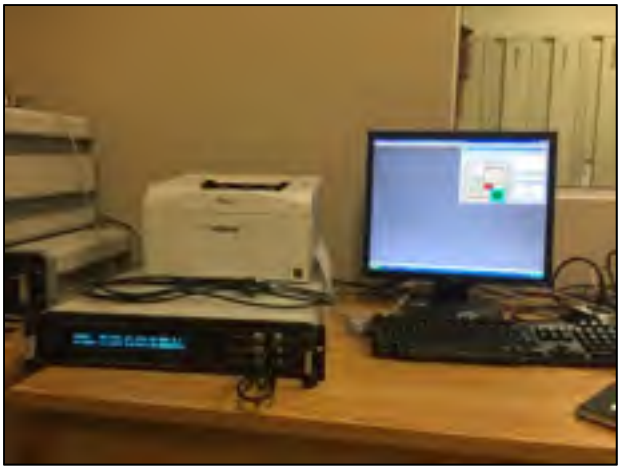

Figure 2.13 Images showing main devices for BDS technique

2.4.7 Four-point probe

The four-point probe test was used to determine the resistivity of a composite materials. A direct current (DC) power source with a high internal resistivity applies a current through two outer electrodes. A voltmeter measures the potential drop between the two inner electrodes, from which the resistivity in the sample can be calculated. The four-point probe test was selected for this measurement due to its ability to correct for material-electrode contact resistance. This increases the reliability of the measurement compared to two-point equivalent tests.

The electrical conductivity of vinyl ester resin/graphene black 3X composites at different loadings were determined using a four-point probe resistivity measurement system (Figure 2.14). Measurements of electrical conductivity were performed using a Keithley 2000 instrument. For measurement of the electrical properties, the composite films were cut to a diameter of 3 cm and a thickness of 1.45 mm. The resistivity of the samples (ρ is the resistivity (Ωcm) was measured in a four-point probe unit using the following equation.

$$\rho = \rho_s . t = \frac{V}{I} . t . \frac{\pi}{\ln 2} . F(\frac{t}{s}) \tag{2.2}$$

$$\text{Conductivity } (\sigma, S/cm) = \frac{1}{\rho} \tag{2.3}$$

Where V is the applied voltage, I is the measured current through the sample, F(t/s) is a correction factor, s is the distance between the probes and s = 2.61 mm.

In this formula *t* is the film thickness, V is the measured voltage and I is the measured current. This gives that the resistivity is independent of the distance *s* between the electrodes. In this experiment, for a value of thickness t = 1.45 mm and s = 2.61 mm, we consider the measurement of body resistivity on thin samples. From the Table 2.5, F(t/s) = 0.9948 with t = 1.45 mm, s = 2.61 mm.

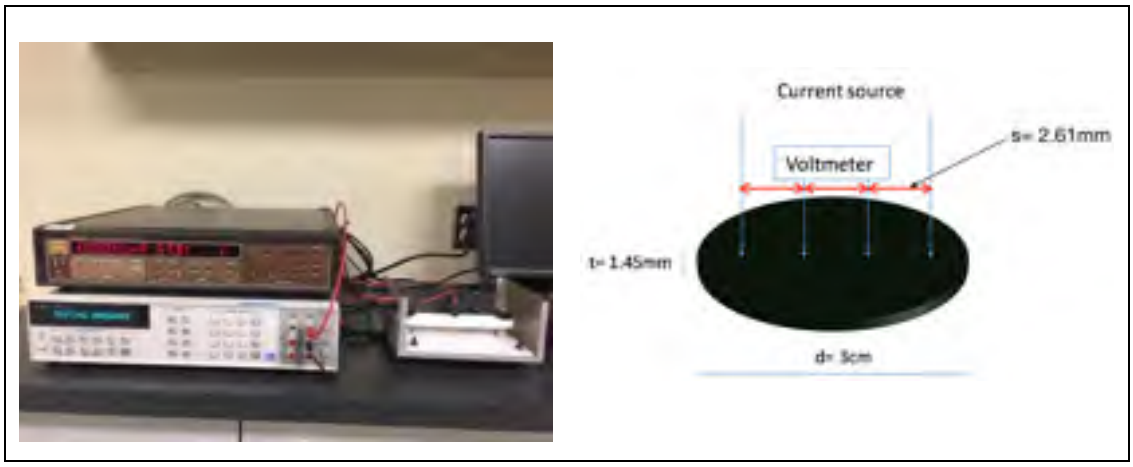

Figure 2.14 Four-point probe collinear probe resistivity method

Table 2.5 Measurement of body resistivity ρ on thin samples of thickness t and spacing s Taken from F.M.Smits (1957)

t/s	F(t/s)
0.4000	0.9995
0.5000	0.9974
0.5555	0.9948
0.6250	0.9898
0.7143	0.9798
0.8333	0.9600
1.0000	0.9214
1.1111	0.8907
1.2500	0.8490
1.4286	0.7938
1.6666	0.7225
2.000	0.6336

CHAPTER 3

RESULTS AND DISCUSSIONS

3.1 Introduction

A nanocomposite material was made via dispersing graphene black 3X into a vinyl ester resin matrix. In this section, results and relevant discussions are presented.

3.2 Results and discussions

3.2.1 Electrical conductivity of 3X and OX graphene under compression

The samples were synthesized using a compressive force to increase the contact, form a cohesive sample body and ensure conductivity. Here, we investigate first the electrical conductivity of a well-known commercial graphene (G/X) containing particles of 3-6 layers thick and another version, named OX graphene. The latter is expected to have higher purity and thinner structure, making it more suitable for advanced technology. The comparison of the electrical conductivity is made between both graphene products in samples of the same mass (1 mg) with equal applied compression at the room temperature.

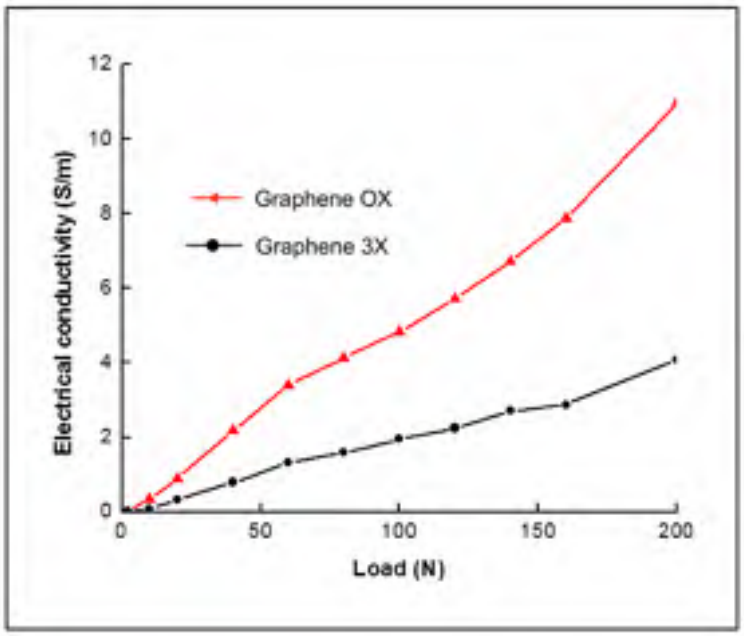

Figure 3.1 Electrical conductivity versus pressure of two types of graphene

The electrical behavior of graphene black 3X and graphene black OX under compression (0.3 to 200 N) is shown in Fig. 3.1. For both types of graphene, the more pressure graphene is applied, the higher the electrical conductivity is observed. Both graphenes show an increase in the electrical conductivity at load 200 N. At a load of 200 N, the electrical conductivity of graphene black 3X and graphene black OX reaches at nearly 4 S/m and ~12 S/m, respectively, meaning that the electrical conductivity of XO is 3 times higher compared to graphene black 3X.

In this master thesis, mechanical, thermal, and electrical properties of graphene black 3X reinforced vinyl ester resin nanocomposites are correlated with topographical features, morphology and dispersion state of graphene.

3.2.2 Morphological studies

a. Morphological investigation using AFM

Atomic Force Microscopy (AFM) is a suitable strategy to describe graphene black 3X by revealing the length and thickness of graphene sheets and layer morphology. For an AFM study of pure graphene, the sample is prepared by scattering graphene in solvents such as acetone or water onto a freshly fractured mica surface and drying.

The dispersion of graphene black 3X sheets in the composite matrix was also investigated by atomic force microscopy (AFM). The topologies of the surface of the graphene black 3X, and the composite films are shown in Figure 3.2. This reveals the average thickness of the graphene black 3X sheets to be around 5 nm (Figure 3.2), indicating well exfoliated nanosheets. With the thickness of single graphene layer of 0.345 nm (one atom thickness), the graphene stacks are estimated to contain 6-8 layers. This is in line with supplied information of the manufacturer NanoXplore of 6-10 layers. Furthermore, surface modification of graphene black 3X was a homogeneous dispersion of individual graphene sheets in the vinyl ester resin matrix on the micrometre area (Figure. 3.3). Combined with images SEM observations, it is seen that the rough surface of the nanocomposite acted a barrier to transport of volatile products created during decomposition process and can enhance the general thermal stability of the polymer matrix. Additionally, the incorporation of graphene black 3X into the matrix created nanoscale roughness which in other cases has been used to give materials superhydrophobic properties (Peng et al., 2018).

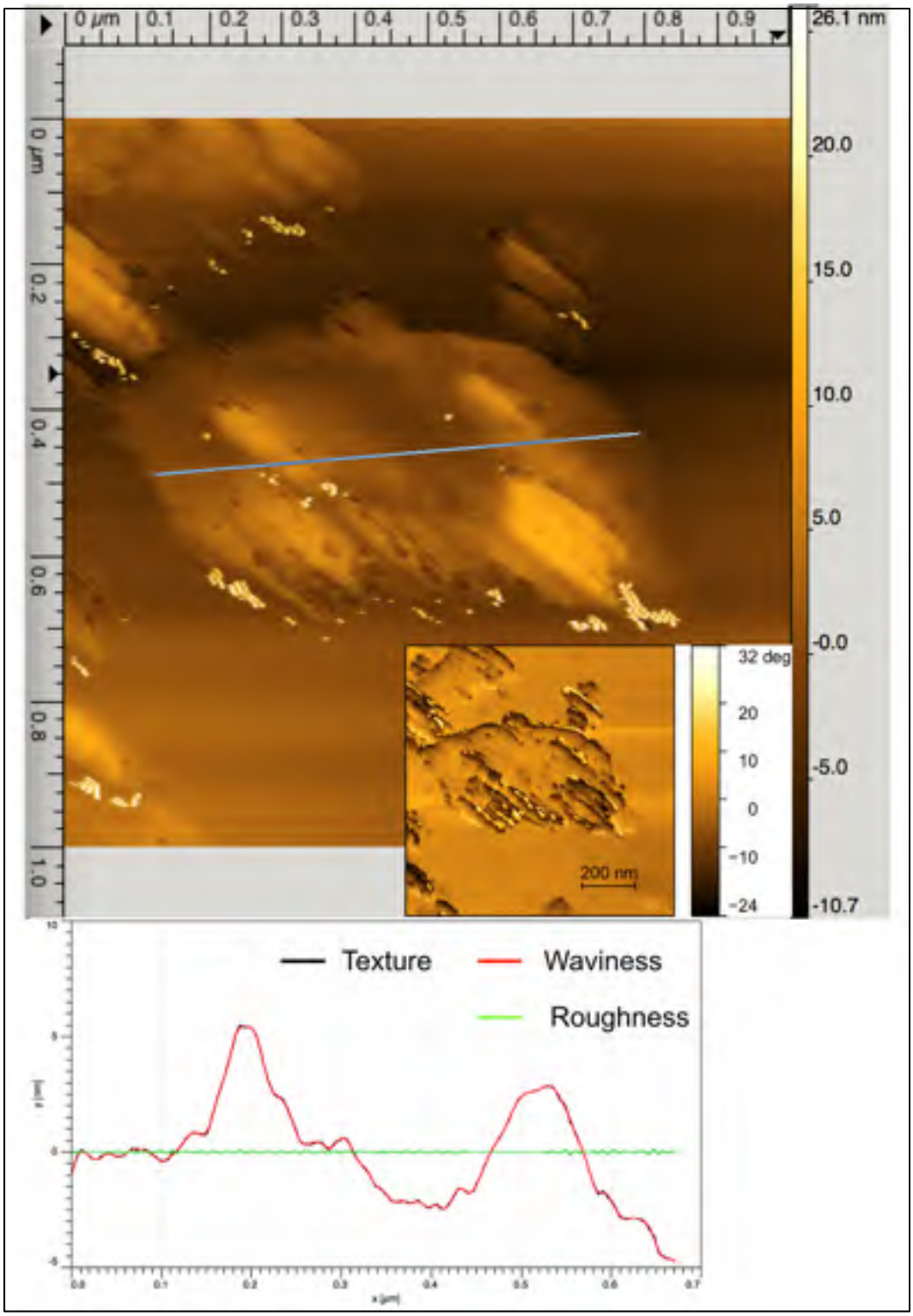

Figure 3.2 AFM image of graphene black 3X with 500x500 nm

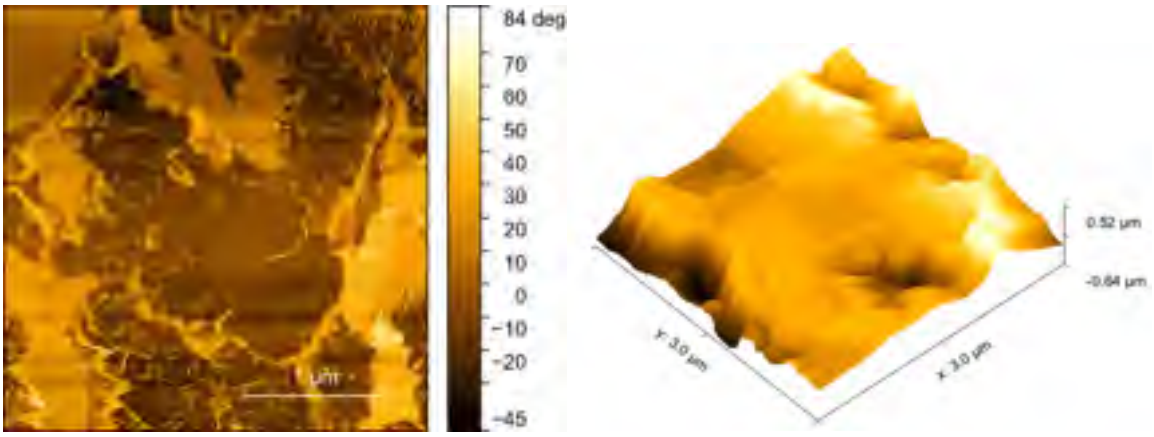

Figure 3.3 AFM images of VSR_20%G with 3x3µm

b. Morphological investigation using SEM

The morphological properties of a polymeric nanocomposite can be changed by incorporation of graphene black 3X in different ratios. The packing arrangement of the polymer may be affected by the dispersion of foreign element in the continuous polymeric matrix, which can cause the formation of voids. In certain cases, the characteristics of the nanocomposite are adversely influenced, which suggests the agglomeration of the particles in the polymeric matrix. Therefore, checking the dispersion of the graphene black 3X in the bulk of the nanocomposite is of great importance to interpreting the results.

The images shown in Figure 3.4 document the distribution of graphene black 3X in the matrix with increasing loading from 1 to 10 wt.%. Figure 3.4a and Figure 3.4b demonstrate an uneven dispersion of graphene in the vinyl ester resin, which takes the appearance of a layered structure compared to the smooth surface of the vinyl ester resin. However, in the other images, the well uniform dispersion of graphene black 3X sheets in the polymer matrix are shown. The images from SEM displays that the distribution of graphene sheets black 3X in the vinyl ester resin is random. This is most evident in the Figure 3.4b with 5 wt.% loading of graphene.

Figure 3.5 shows the SEM of graphene black 3X to be a layered, occasionally folded structure. The thickness of these layered graphene sheets is measured to be 119 nm and 471 nm in folded areas (Figure 3.5a). This is in contrast to the dispersed graphene sheets measured by AFM to have a thickness between 43 nm to 73 nm as shown in Figure 3.5b. This phenomenon of a few restacking may affect the tensile properties and other characteristics of the composites. By SEM, the width of a graphene sheets can be measured to be between 10.6 μm to 17.5 μm as shown in Figure 3.5c and Figure 3.5d. These SEM results reveal that the compatibility of graphene black 3X with the resin was enhanced as the proportion of carbon black in the polymer matrix increased. Through a random distribution of cross-linked graphene sheets, a nanocomposite can be formed with the characteristic properties of the graphene such as enhanced electrical conductivity and mechanical properties.

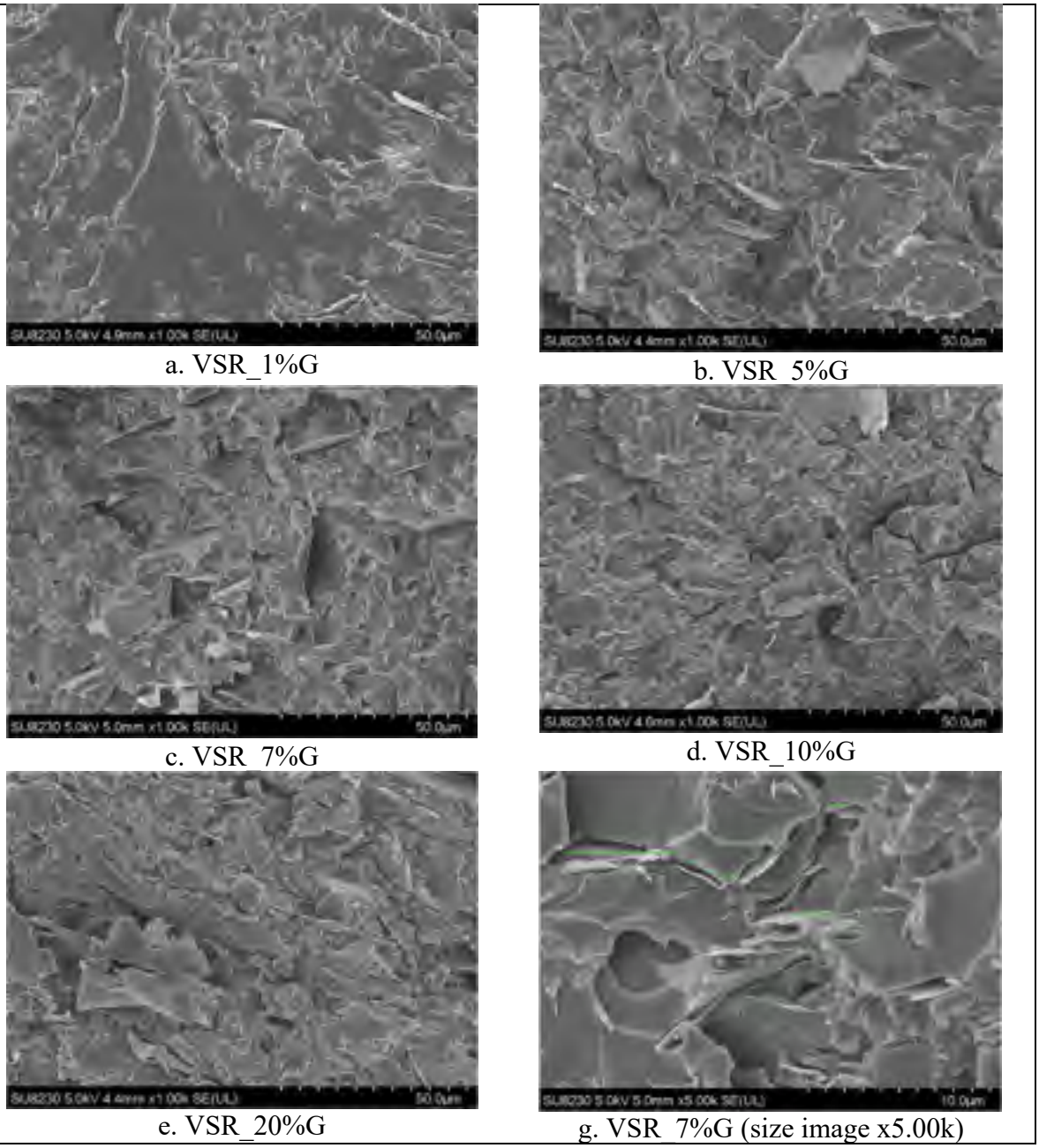

a. VSR_1%G

b. VSR_5%G

c. VSR_7%G

d. VSR_10%G

e. VSR_20%G

g. VSR_7%G (size image x5.00k)

Figure 3.4 SEM images of cross section of the composites
a. VSR_1%G, b. VSR_5%G, c. VSR_7%G, d. VSR_10%G,
e.VSR_20%G, and g. VSR_7%G (size image x5.00k) respectively

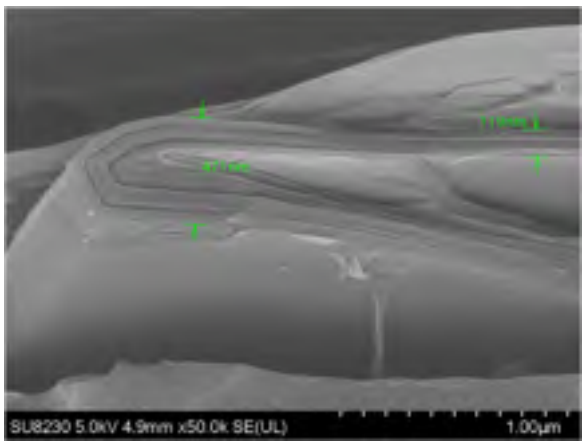

a. The graphene layer is folded

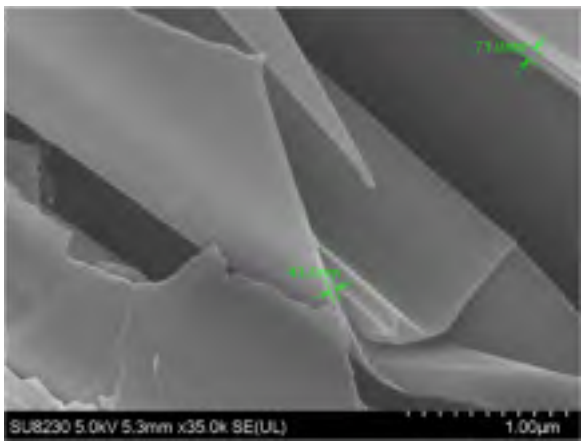

b. The thickness of graphene layers

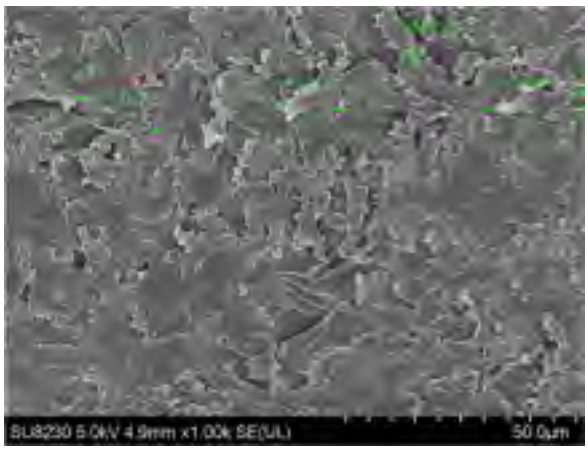

c. The width of graphene layers

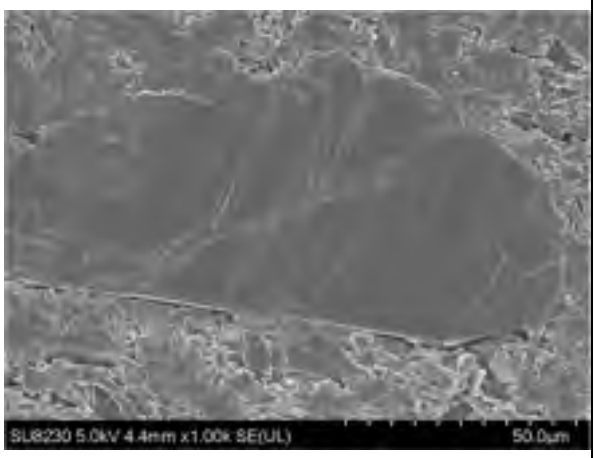

d. The images of 1 graphene sheet

Figure 3.5 SEM images of structure characteristics of black 3X graphene in vinyl ester matrix a. graphene layer is folded, b. c. thickness and width of graphene layers, and d. the graphene sheet

3.2.3 Thermal properties

The effect of the addition of graphene black 3X on the thermal degradation of vinyl ester resin was studied by thermogravimetric analysis (TGA). TGA curves for vinyl ester resin with hardener resin (VSR_H), vinyl ester resin with varying amounts of graphene 3X loading (VSR X%G), and graphene black 3X (G3X) are shown in Figure 3.6 with corresponding data being summarized in Table 3.1.

From the TGA curve of VSR_H, the initial weight loss occurs at temperature of 400 °C (Figure 3.6 (VSR_H)). The most dramatic weight loss, starting from 350 °C, corresponds to the degradation of the backbone chain (CH_2 groups) in polymer (Bora et Dolui, 2012; Costache, Jiang et Wilkie, 2005; Sabet, Soleimani et Hosseini, 2018; Wu, Zhao et Chen, 2012). The second mass loss begins at 580°C and is related to the evaporation of resin in the composite matrix. When the temperature reaches to 700 °C, the residual weight is approaching 0 %, meaning that the resin is almost entirely decomposed. Graphene black 3X plays an important role in the thermostability of the composites. On incorporation of graphene black 3X, the major degradation temperature of vinyl ester resin was remarkably improved from 170-230 °C (Figure 3.5a). This improvement in thermal stability is attributed to the strong interaction between graphene black 3X and vinyl ester resin which stabilizes the polymer segments at the interfaces of vinyl ester resin and graphene 3X. The incorporation of graphene into the matrix acts as a mass transport barrier to the volatile products generated during decomposition which may enhance the overall thermal stability of the composite.

The results of the differential thermal analysis (DTA) of the vinyl ester resin composites with graphene black 3X display two-step thermal degradation as shown in Figure 3.7. Consistent with the TGA results, the primary degradation begins at 420°C. Interestingly, it is observed that with higher loading of graphene the decomposition shifts to slightly lower temperatures. However, the decomposition temperature plummeted in first phase when there was no enhancement of graphene in the resin film. As considered by Figure 3.6 and Figure 3.7, the addition of graphene black 3X slightly increases the thermal endurance of the composites. Table 3.1 demonstrates that increasing the percentage of graphene substance will improve the thermal properties of the nanocomposite materials.

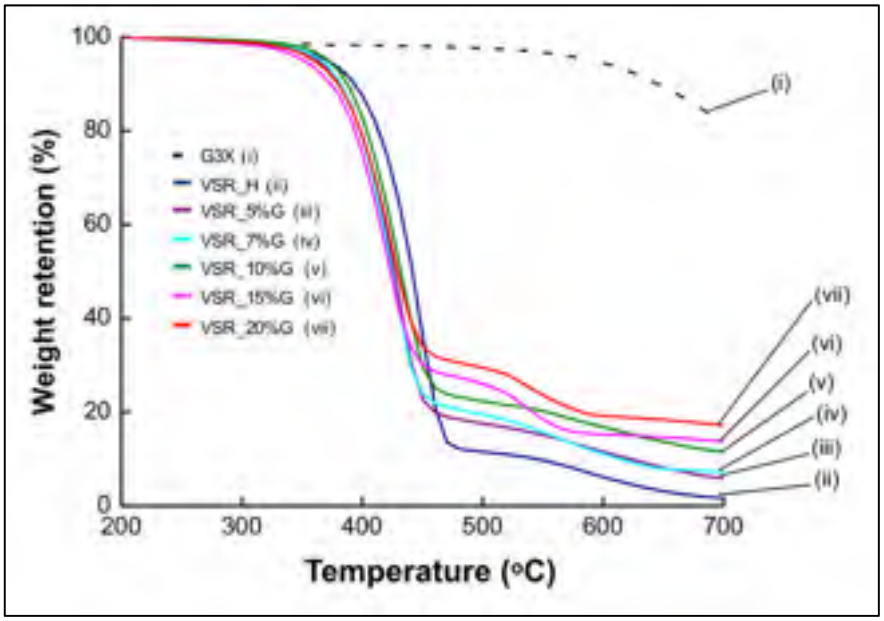

Figure 3.6 TGA curves of neat G3X, neat resin and VSR/G3X composites

Table 3.1 TGA data of prepared samples

Sample	Major degradation temperature (T_d) °C	Weight loss % at temperature				Weight retention (%) at 700°C
		350°C	450°C	500°C	600°C	
VSR_H	410	2	34	88	94	1
VSR_5%G	365	4	79	83	89	5
VSR_7%G	380	3	75	80	89	7
VSR_10%G	385	3	73	78	83	11
VSR_15%G	385	5	70	74	85	14
VSR_20%G	390	4	67	70	81	18
G3X	550	1	2	3	5	82

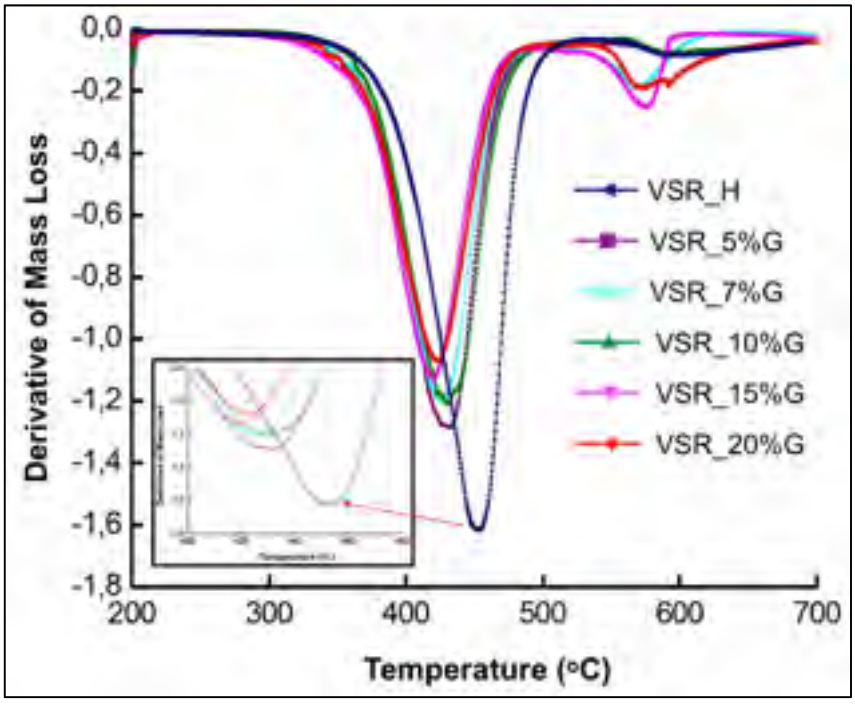

Figure 3.7 DFA thermograms of the derivative of mass loss as a function of temperature

3.2.4 Mechanical properties

In many applications of coatings, mechanical stability is required for the protection of the substrate. Due to the large particle aspect ratio and outstanding mechanical theoretical strength, the graphene black 3X reinforcement of vinyl ester resin shows a significant impact on the mechanical properties of the composites. The representative stress-strain curves of the composites at various graphene loadings are shown in Figure 3.8. The measured improvement is observed to be dependent on the graphene content. For 5 wt% loading, the primary improvement is in the ultimate strain. However, for higher graphene contents, the composites exhibit a significant increase in ultimate tensile strength. Even at as little as 7 wt.% graphene the tensile strength is 1.5 times as higher than 5 wt.%, demonstrating the importance of the dispersion of the graphene particles, as observed in the SEM results (Figure 3.4g). Additions up to 20% graphene demonstrate significant increases in the ultimate strain up to 3.5 mm/mm.

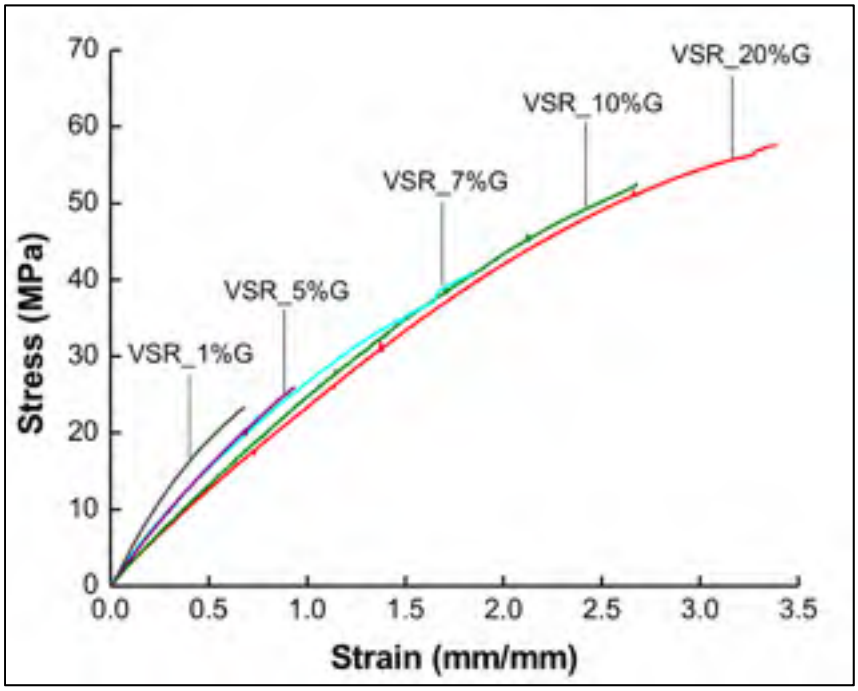

Figure 3.8 Representatives stress-strain curves of the composites with different graphene black 3X contents

Table 3.2 The tensile strength of the nanocomposites

% of Graphene black 3X	Ultimate Tensile strength (MPa)
1	23.34 ± 1.95
5	26.00 ± 1.93
7	40.87 ± 1.15
10	52.71 ± 0.10
20	57.63 ± 0.76

The dependence of the ultimate tensile strength on the filler content of graphene is shown in Table 3.2. For the loading of graphene black 3X at 1 % or 5 wt.%, the tensile strength of the nanocomposite remains almost constant. However, further additions of graphene black 3X led to significant increase of the tensile strength of the nanocomposites. The maximum value of tensile strength was achieved to about 57.6 MPa with a graphene back 3X content of 20 wt.%, an improvement by over a factor of two.

3.2.5 Electrical properties

a. Four-point probe test

The electrical conductivity of vinyl ester resin/graphene black 3X composites at different graphene contents are determined using a four-point probe resistivity measurement system as shown in Figure 3.9. This figure shows that composites with at least 7 % of G3X exhibit some degree of electrical conductivity with constant conductivity for current intensities up to 5 mA. Moreover, the electrical conductivity increases with the of graphene content in the formulations. The samples containing 20 wt.% of G3X demonstrate the highest conductivity tested of about 3.7 10^{-2} S/cm. Increasing higher conductivity with content is explained by the increased probability of favorable electrical contacts between graphene particles dispersed homogeneously in the resin matrix.

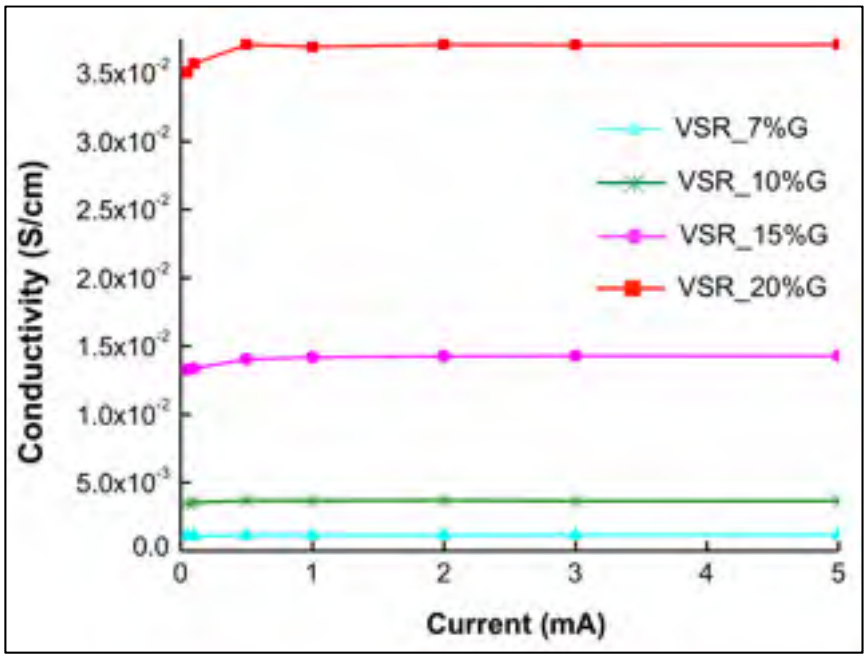

Figure 3.9 Electrical properties by four point probe test of VSR_G3X

b. Broadband dielectric spectroscopy

The electrical conductivity of vinyl ester resin-graphene black 3X nanocomposites as a function of frequency-domain dielectric responses is shown in Figure 3.10 and Figure 3.11, in terms of modulus of the complex conductivity. The measurements were recorded from 10^{-2} to 30 kHz frequency at room temperature.

The vinyl ester resin containing 3 - 20 wt.% of graphene black 3X featured a percolation threshold concentration at about 5 wt.% which represents a dominance of the electrical conduction over dielectric response in the frequency range. The dielectric response of vinyl ester resin with 5% graphene loading (VSR_5% G) exhibited high frequency-independent dielectric losses. Meanwhile, resin with 7% graphene (VSR_7% G) demonstrated electrical conductivity breakthrough, exposing the high-frequency property. At 5 wt.% of G3X, the nanocomposites had an alternating current conductivity over 10^{-8} S/cm at 0.01 Hz as shown in Figure 3.10. When the concentration rises above the percolation threshold, the conductivity increases rapidly.

Figure 3.11 presents the value of the vinyl ester resin sample with the hardener (VSR_H), with 1% graphene (VSR_1%G), and with 3% (VSR_3%G). At low filler concentration, the dielectric response of graphene 3X and vinyl ester resin composite is measured to be under 10^{-15} S/cm and the vinyl ester resin pure is 10^{-17} S/cm. This demonstrates the range of improvement possible with additions of graphene to the resin matrix.

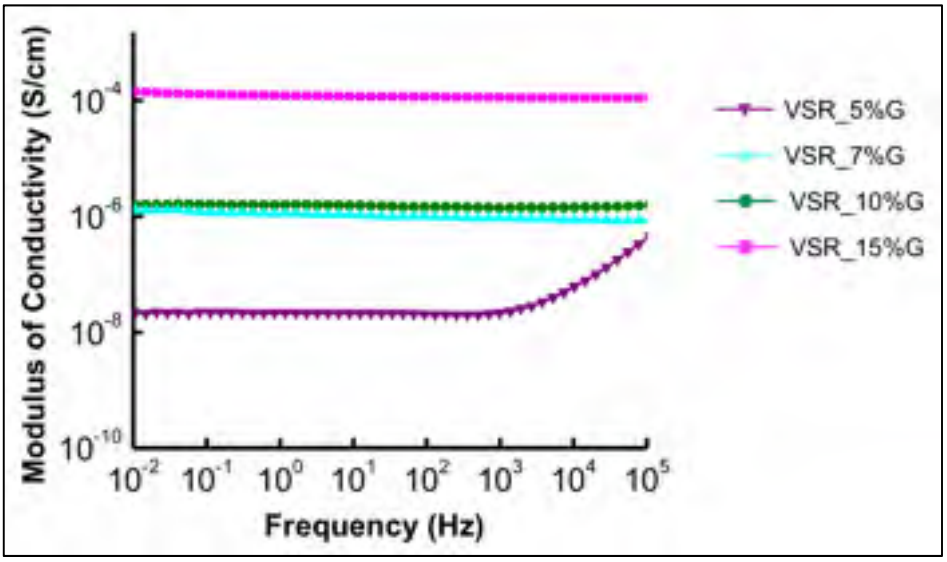

Figure 3.10 Modulus of VSR_G3X complex conductivity as function of frequency

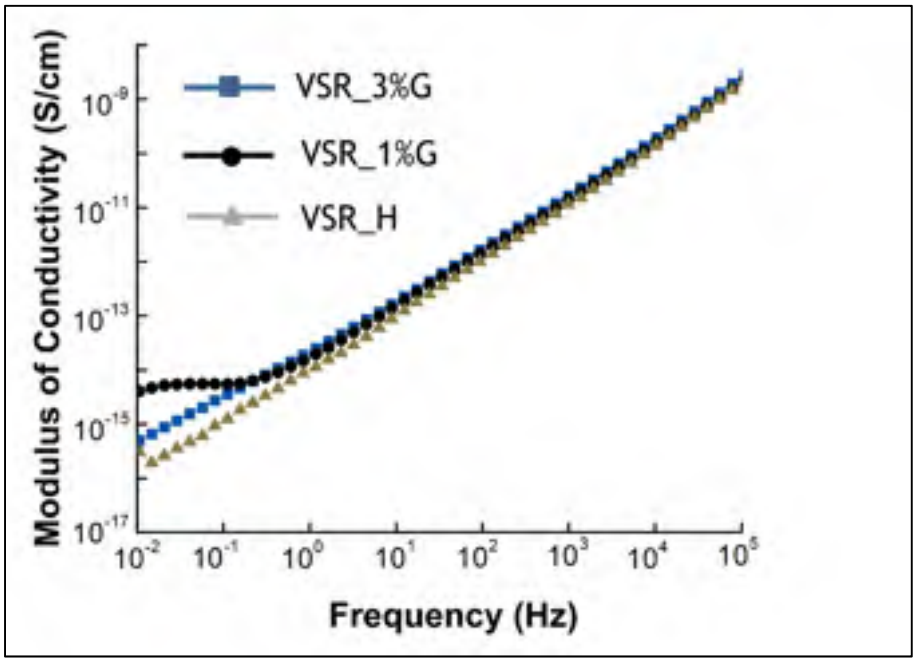

Figure 3.11 Modulus of VSR_G3X complex conductivity as function of frequency VSR_H, VSR_1%G and VSR_3%G

CONCLUSION

The objective in this master thesis is to advance a new nanocomposite material through the process of mixing graphene black 3X with Vinyl ester resin matrix. Apart from the investigation into the characterization of the synthesized samples, the writing also provides a central focus on the optimal preparation of graphene based vinyl ester resin nanocomposite. Some particular properties of importance are exhibited by these novel materials including improved thermal stability, enhanced mechanical strength and electrical conductivity. The success of incorporating graphene into the polymer matrix is observed in the morphological analyses by SEM and AFM.

In the first chapter of the thesis, the theoretical foundation for the work was explained and a literature review provided a background on thermoset resins, vinyl ester resin, graphene, and relevant characterization methods. Chapter 2 presented an in-depth review of the materials and methods utilized in this work. The specific materials, synthesis method, characterization techniques and testing procedures involved in the making and analysis of graphene vinyl ester resin composite were explained to clarify the experiments conducted for this thesis.

Chapter 3 provides the results of those tests indicating a beneficial combination of properties for composites of graphene and vinyl ester resin. By incorporating black 3X graphene particles into a resin matrix, it is possible to fabricate low graphene content conductive coatings with improved thermal stability. TGA analysis shows that these nanocomposites can be used at a temperature lower than 300ºC without any chemical decomposition. Electrically conductive coatings can be achieved with the addition of only 5 % of graphene. The highest value of conductivity was 3.7. 10^{-2} S/cm with 20 wt.% of G3X, high enough to various electrical devices. Furthermore, it was observed that the mechanical properties can be increased by a factor of two. This combination of improvements in both mechanical stability and electrical functionalization is exceptional and suggests a future for this type of graphene thermoset nanocomposite in a variety of applications.

RECOMMENDATIONS

Although the preliminary results issued in this work are encouraging, there remains several open questions for future work to explore. For example:

a. What are chemical interactions at the graphene/resin interface?
b. What is the real distribution of graphene in the resin matrix?
c. How to improve the dispersion of fillers and thus reduce the filler content to achieving the similar performance (electrical, thermal, mechanical properties).

The BisPhenol A (BPA) containing epoxy-vinyl ester resin used in this work has a negative impact on the environment, so there is significant interest in replacing this by a green-sourced or high recyclability alternative. This is the motivation behind planning similar investigations of nanocomposites based on a bioepoxy resin (bio-resource resin). However, this dispersion of the graphene in the bioepoxy was difficult with current laboratory fabrication methods. Preliminary results which formed an insulating composite even at high graphene content are included in the Appendix.

It is expected that bio-based polymer composite products will be available in the market based on this technique in the upcoming years. However, the study of mechanisms related to the production and functionalization of graphene nanomaterials will continue to require more research to generate sustainable products for the global market.

APPENDIX I

COMPLEMENTARY MEASUREMENTS

a. Results of Vinyl ester resin, Graphene black 3X, Hardener MEKP, and Vinyl ester resin/Graphene black 3X composites were obtained from FTIR-spectrum and FTIR-time base experiment

FTIR spectra of pure Vinyl ester resin, graphene, and VSR/G3X resin composite are shown in Fig.-A I-1 and Fig.-A I-2. From the FTIR spectrum, it is seen that the absorption peaks for O-H deformation, C-OH stretching vibration, C-O stretching vibrations and carbonyl group (C=O). From the FTIR results, we can say that graphene black OX has been successfully incorporated or not in the polymer matrix.

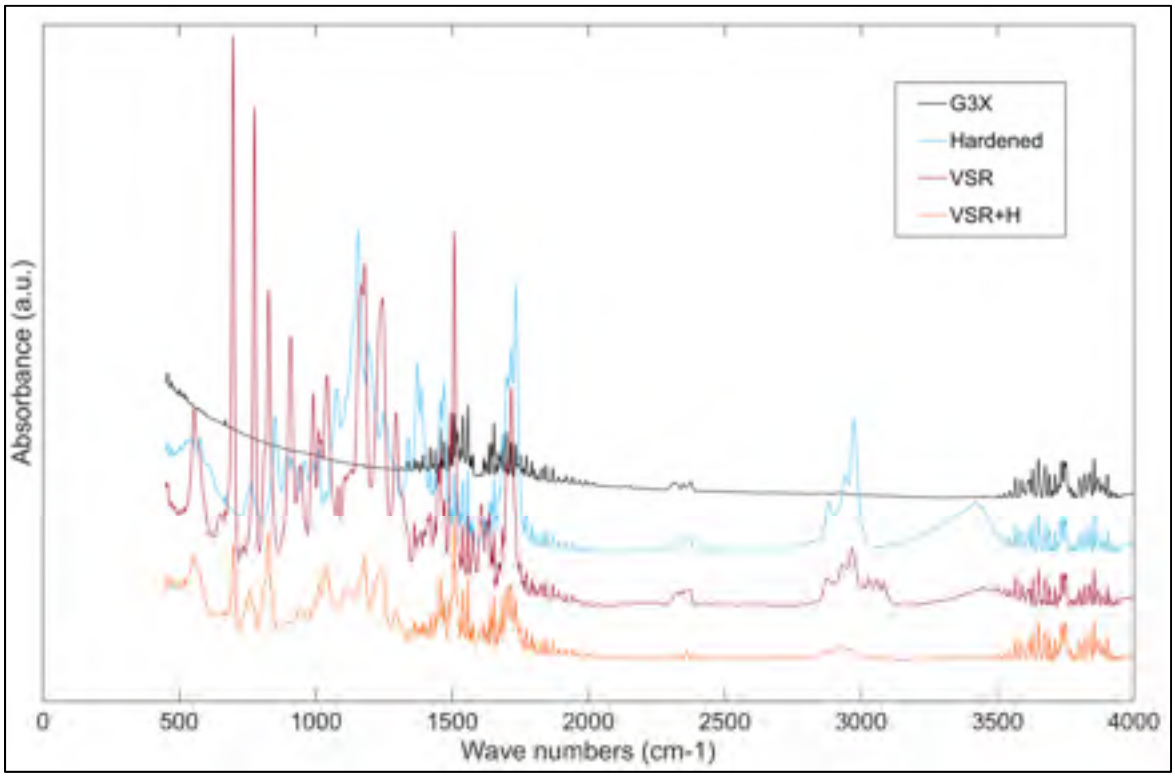

Figure-A I-1 FTIR –spectrum patterns of Graphene black 3X, Hardener MEKP, Vinyl ester resin and Vinyl ester resin/MEKP mixture

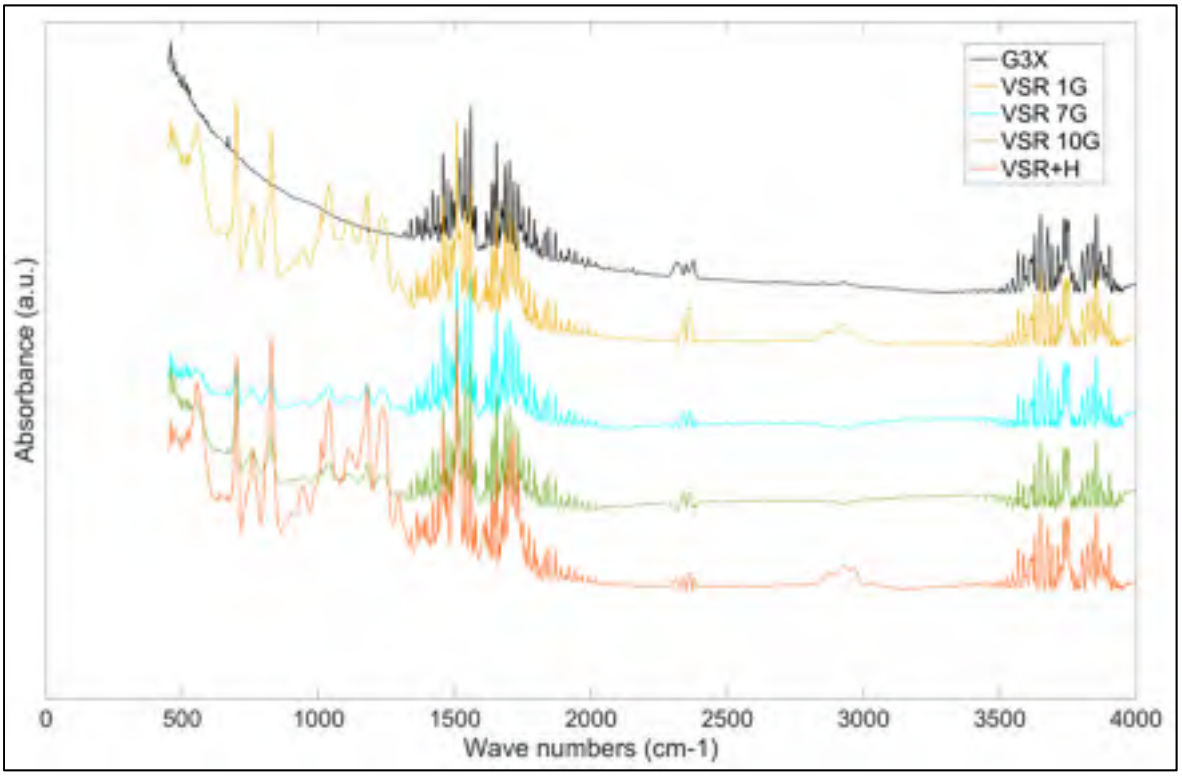

Figure-A I-2 Comparison of model and experimental data for Vinyl ester resin Graphene black 3X composites with different filler loadings

b. Bio-epoxy resin/graphene black OX

1. Bio-epoxy resin and graphene black OX datasheet

The bio-epoxy resin and hardener was supplied by Entropy Resins, Inc and the designation codes and characteristics of the materials are shown in Table-A I-1 as following technical information Entropy Resins Inc. 2015.

Table-A I-1 Characteristics of the bio-epoxy and hardener resins

Product (Bio-epoxy/Hardener)	**Super Sap CPM epoxy/Super Sap CPF hardener**
Key features	Excellent adhesion, high modulus, good elongation
Applications	Compression molding
Potetial use	Snowboard, Skateboard, Ski
Mix ratio (by weight)	100:43
Biobased carbon content (ASTM D6866)	30%
Component density (specific density @ 25°C)	1.14 (epoxy), 0.98 (hardener)

All technical information of graphene black OX is based on NanoXplore (Canada) Technical datasheet. Table-A I-2 and Table-A I-3 illustate the physical and chemical properties of graphene black OX as following the NanoXplore technical data sheet.

Table-A I-2 Physical properties of graphene black OX

Property	**Value**
Particle size (laser diffraction)	D_{50}= 13 µm
Number of layers	6-10
Bulk density	0.14g/cm^3
Solubility	Insoluble
Moisture (TGA)	<0.6 wt%
Peak decomposition temperature	774°C

Table-A I-3 The graphene black OX chemical composition values of the chemical element

Element	Value
Carbon	>95 at.%
Oxygen	3.5 at.%
Sulfur	0.25 at.%
Metal impurities	<1 at.%

2. Morphological investigation using AFM

The Figure-A I-3 represents the dispersion of graphene sheets in the matrix of bio-epoxy resin with the image size 5x5 µm by using the AFM tapping mode. In the AFM image of Bio_10%GOX, the average roughness of the topology was found to be around 20 nm (Fig.-A I-3c). The image shows a smooth surface appears and the rest of the image illustrates the graphene black OX dispersed in the matrix polymer. Therefore, the distribution of graphene black OX in the resin is not uniform well in the bio-epoxy matrix.

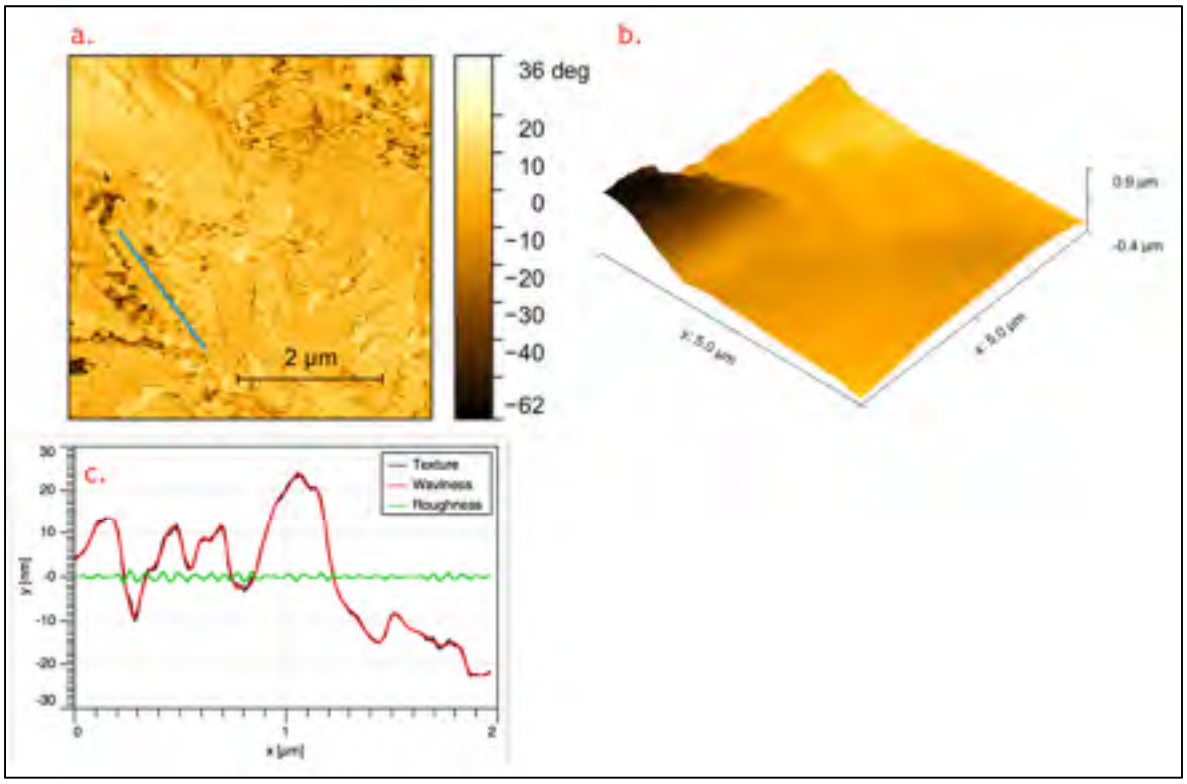

Figure-A I-3 AFM images of Bio_10%GOX with 5x5 µm

3. Morphological investigation using SEM

The surface characteristics of bio-epoxy resin/graphene black OX were investigated using SEM with 20 wt.% and 25 wt.% loading of graphene black OX, respectively. The images demonstrate two main reasons for poor compatibility of GOX into bio-resin matrix:

- The same blending and curing procedures were utilized as in the vinyl ester resin/graphene black 3X composites. However, air holes are visible in the matrix as shown in Fig.-A I-4c. Appearance of this air holes indicates poor incorporated graphene black OX in the bio matrix.
- Fig.-A I-4a and Fig.-A I-4b illustrate two different areas of bio resin matrix at the loading of 25 wt.% graphene black OX. Fig.-A I-4a shows that graphene black OX has been successfully dispersed in the bio-epoxy matrix. However, in the second area most of the region is covered with bio-epoxy resin. Furthermore, it also revealed that the dispersion of graphene black OX is not uniform to create the homogeneous pathway of graphene layers in the matrix.

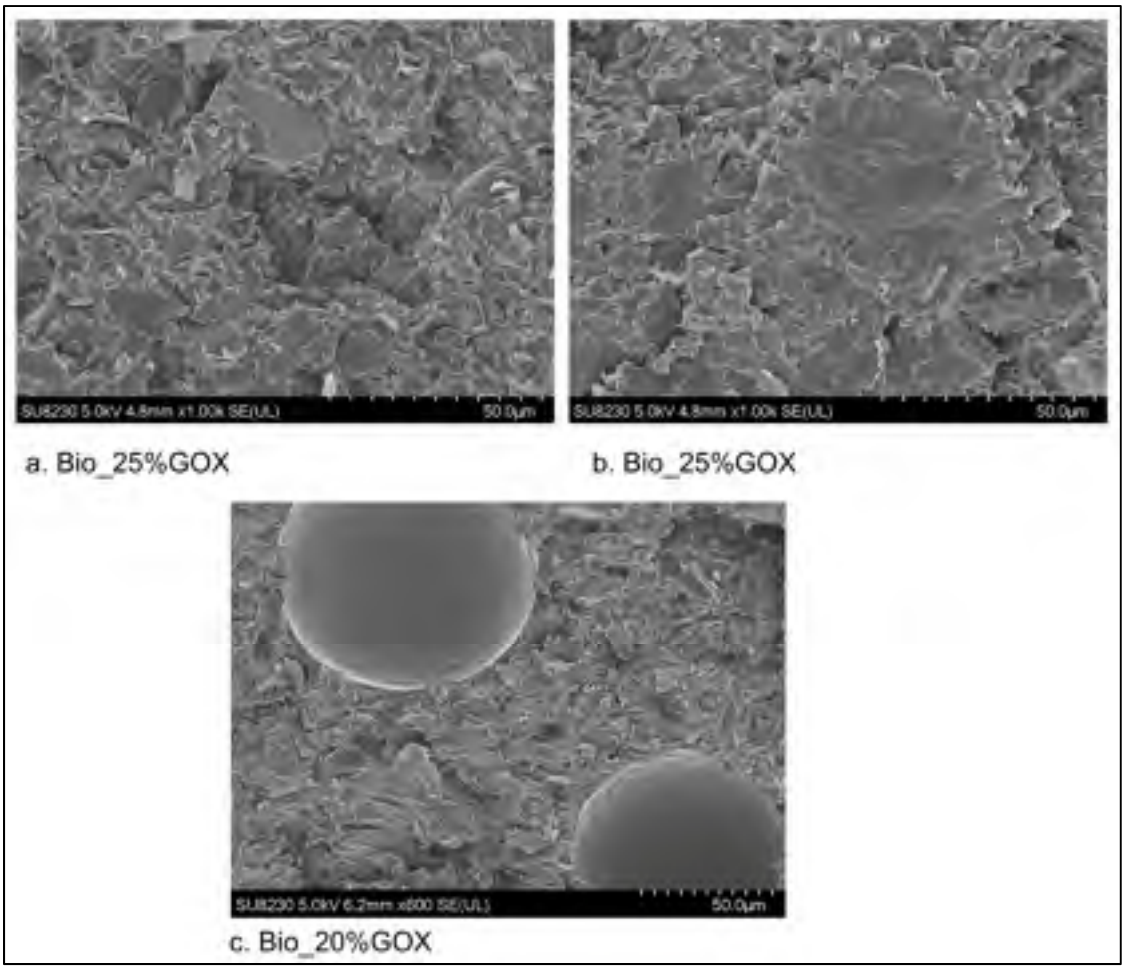

Figure-A I-4 SEM images of cross section of the composites a., b. Bio_25%GOX, respectively, c. Bio_20%GOX

BIBLIOGRAPHY

Abdin, Z., M. A. Alim, R. Saidur, M. R. Islam, W. Rashmi, S. Mekhilef et A. Wadi. 2013. « Solar energy harvesting with the application of nanotechnology ». *Renewable and Sustainable Energy Reviews,* vol. 26, p. 837-852.

Aghili, Vahid Arablia and Alireza. 2016. *Graphene oxide/vinyl ester resin nanocomposite: the effect of graphene oxide, curing kinetics, modeling, mechanical properties and thermal stability*.

Agnihotri, Nidhi, Ankan Dutta Chowdhury et Amitabha De. 2015. « Non-enzymatic electrochemical detection of cholesterol using β-cyclodextrin functionalized graphene ». *Biosensors and Bioelectronics,* vol. 63, p. 212-217.

Aguilar-Bolados, Héctor, Miguel A. Lopez-Manchado, Justo Brasero, F. Avilés et Mehrdad Yazdani-Pedram. 2016. « Effect of the morphology of thermally reduced graphite oxide on the mechanical and electrical properties of natural rubber nanocomposites ». *Composites Part B: Engineering,* vol. 87, p. 350-356.

Al-Saleh, Mohammed H., et Uttandaraman Sundararaj. 2011. « Review of the mechanical properties of carbon nanofiber/polymer composites ». *Composites Part A: Applied Science and Manufacturing,* vol. 42, nº 12, p. 2126-2142.

Almajid, A., L. Sorochynska, K. Friedrich et B. Wetzel. 2015. « Effects of graphene and CNT on mechanical, thermal, electrical and corrosion properties of vinylester based nanocomposites ». *Plastics, Rubber and Composites,* vol. 44, nº 2, p. 50-62.

Andreas Kandelbauer, Gianluca Tondi, Oscar C. Zaske, Sidney H. Goodman. 2013. *Unsaturated polyesters and vinyl esters*. Handbook of thermoset plastics.

Anupama Chaturvedi, Ashutosh Tiwari, Atul Tiwari. 2013. « Spectroscopic and morphological analysis of graphene vinylester nanocomposites ».

Archie, G. E. 1942. « The Electrical Resistivity Log as an Aid in Determining Some Reservoir Characteristics ». *Transactions of the AIME,* vol. 146, nº 01, p. 54-62.

Atta, Ayman M., Shymaa M. El-Saeed et Reem K. Farag. 2006. « New vinyl ester resins based on rosin for coating applications ». *Reactive and Functional Polymers,* vol. 66, nº 12, p. 1596-1608.

Azeez, Asif Abdul, Kyong Yop Rhee, Soo Jin Park et David Hui. 2013. « Epoxy clay nanocomposites – processing, properties and applications: A review ». *Composites Part B: Engineering,* vol. 45, nº 1, p. 308-320.

Azizi, Sohrab, Eric David, Michel F. Fréchette, Phuong Nguyen-Tri et Claudiane M. Ouellet-Plamondon. 2018. « Electrical and thermal conductivity of ethylene vinyl acetate composite with graphene and carbon black filler ». *Polymer Testing,* vol. 72, p. 24-31.

Beckman, Eric. 2018. « The world of plastics, in numbers ».

Biron, M. 2018. *Thermoplastics and thermoplastic composites*.

Bkakri, R., A. Sayari, E. Shalaan, S. Wageh, A. A. Al-Ghamdi et A. Bouazizi. 2014. « Effects of the graphene doping level on the optical and electrical properties of ITO/P3HT:Graphene/Au organic solar cells ». *Superlattices and Microstructures,* vol. 76, p. 461-471.

Bolotin, K. I., K. J. Sikes, Z. Jiang, M. Klima, G. Fudenberg, J. Hone, P. Kim et H. L. Stormer. 2008. « Ultrahigh electron mobility in suspended graphene ». *Solid State Communications,* vol. 146, nº 9, p. 351-355.

Bora, C., et S. K. Dolui. 2012. « Fabrication of polypyrrole/graphene oxide nanocomposites by liquid/liquid interfacial polymerization and evaluation of their optical, electrical and electrochemical properties ». *Polymer,* vol. 53, nº 4, p. 923-932.

Broido, A. 1969. « A simple, sensitive graphical method of treating thermogravimetric analysis data ». *Journal of Polymer Science Part A-2: Polymer Physics,* vol. 7, nº 10, p. 1761-1773.

C Berthomieu, R Hienerwadel. 2009. « Fourier transform infrared (FTIR) spectroscopy ».

Cantor, Kirk M., et Patrick Watts. 2011. « 1 - Plastics Materials ». In *Applied Plastics Engineering Handbook*, sous la dir. de Kutz, Myer. p. 3-5. Oxford: William Andrew Publishing.
< http://www.sciencedirect.com/science/article/pii/B9781437735147100017 >.

Castro Neto, A. H., F. Guinea, N. M. R. Peres, K. S. Novoselov et A. K. Geim. 2009. « The electronic properties of graphene ». *Reviews of Modern Physics,* vol. 81, nº 1, p. 109-162.

Changgu Lee, Xiaoding Wei, Jeffrey W. Kysar, James Hone. 2008. « Measurement of the Elastic properties and intrinsic strength of monolayer graphene ». *Science*.

Changwoon Jang, Thomas E. Lacy, Steven R. Gwaltney, Hossein Toghiani, and Charles U. Pittman Jr. 2012. « Relative reactivity volume criterion for cross-linking: Application to vinyl ester resin molecular dynamics simulations ».

Chenlu Bao , Lei Song , Weiyi Xing ,Bihe Yuan ,Charles A. Wilkie , Jianliu Huang,Yuqiang Guoa and Yuan Hu. 2012. « Preparation of graphene by pressurized oxidation and multiplex reduction and its polymer nanocomposites by masterbatch-based melt blending ». *Journal of Materials Chemistry*.

CI. 1999. *The role of monomeric and dimeric oligomers of methyl ethyl ketone peroxide in the cure of unsaturated resin formulations*. International Conference Proceedings: Composites Institute.

Compton, Owen C., et SonBinh T. Nguyen. 2010. « Graphene Oxide, Highly Reduced Graphene Oxide, and Graphene: Versatile Building Blocks for Carbon-Based Materials ». *Small,* vol. 6, nº 6, p. 711-723.

Costache, Marius C., David D. Jiang et Charles A. Wilkie. 2005. « Thermal degradation of ethylene–vinyl acetate coplymer nanocomposites ». *Polymer,* vol. 46, nº 18, p. 6947-6958.

Council, American Chemistry. 2005. *How plastics are made*. Plastics Industry Producer Statistics Group.

D Gay, SV Hoa. 2007. *Composite materials: design and applications*.

D Hull, TW Clyne. 1996. *An introduction to composite materials*.

Doyle, CD. 1961. « Kinetic analysis of thermogravimetric data ».

Dreyer, Daniel R., Sungjin Park, Christopher W. Bielawski et Rodney S. Ruoff. 2010. « The chemistry of graphene oxide ». *Chemical Society Reviews,* vol. 39, nº 1, p. 228-240.

Drobny, JG. 2014. « Handbook of thermoplastic elastomers ».

Dubois, J. Harry. 1900-1975. *J. Harry Dubois Collection on the History of Plastics*.

E Malic, A Knorr. 2013. *Graphene and Carbon nanotubes: ultrafast optics and relaxation dynamics*.

Evanoff Jr., David D., et George Chumanov. 2005. « Synthesis and Optical Properties of Silver Nanoparticles and Arrays ». *ChemPhysChem,* vol. 6, nº 7, p. 1221-1231.

F Kremer, A Schönhals. 2012. *Broadband dielectric spectroscopy*.

F.M.Smits. 1957. « Measurement of sheet resistivity with the Four-Point Probe ».

Faccio, Ricardo, Pablo A. Denis, Helena Pardo, Cecilia Goyenola et Álvaro W. Mombrú. 2009. « Mechanical properties of graphene nanoribbons ». *Journal of Physics: Condensed Matter,* vol. 21, nº 28, p. 285304.

Fang, Ming, Kaigang Wang, Hongbin Lu, Yuliang Yang et Steven Nutt. 2009. « Covalent polymer functionalization of graphene nanosheets and mechanical properties of composites ». *Journal of Materials Chemistry,* vol. 19, nº 38, p. 7098-7105.

Frank, I. W., D. M. Tanenbaum, A. M. van der Zande et P. L. McEuen. 2007. « Mechanical properties of suspended graphene sheets ». *Journal of Vacuum Science & Technology B: Microelectronics and Nanometer Structures Processing, Measurement, and Phenomena,* vol. 25, nº 6, p. 2558-2561.

Gadipelli, Srinivas, et Zheng Xiao Guo. 2015. « Graphene-based materials: Synthesis and gas sorption, storage and separation ». *Progress in Materials Science,* vol. 69, p. 1-60.

García, Ricardo, et Rubén Pérez. 2002. « Dynamic atomic force microscopy methods ». *Surface Science Reports,* vol. 47, nº 6, p. 197-301.

Gaur, Shipra Jaswal and Bharti. 2014. « New trends in vinyl ester resins ».

Geim, A. K. 2009. « Graphene: Status and prospects ». *Science*.

Georgakilas, Vasilios. 2014. *Functionalization of graphne*.

Giessibl, Franz J. 2003. « Advances in atomic force microscopy ». *Reviews of Modern Physics,* vol. 75, nº 3, p. 949-983.

Gómez-Navarro, Cristina, Marko Burghard et Klaus Kern. 2008. « Elastic Properties of Chemically Derived Single Graphene Sheets ». *Nano Letters,* vol. 8, nº 7, p. 2045-2049.

Goyal, Vivek, et Alexander A. Balandin. 2012. « Thermal properties of the hybrid graphene-metal nano-micro-composites: Applications in thermal interface materials ». *Applied Physics Letters,* vol. 100, nº 7, p. 073113.

Gregory, R.V., Kimbrell, W.C., Kuhn, H.H., 1991, Electrically Conductive Non-Metallic Textile Coatings, J. of Coated Fabrics, 20, p.167-175.

Guo, Zhanhu; Ng, Ho Wai; Yee, Gary L.; Hahn, H. Thomas. 2009. « Differential Scanning Calorimetry Investigation on Vinyl Ester Resin Curing Process for Polymer Nanocomposite Fabrication ».

Hamidinejad, S. M., R. K. M. Chu, B. Zhao, C. B. Park et T. Filleter. 2018. « Enhanced Thermal Conductivity of Graphene Nanoplatelet-Polymer Nanocomposites

Fabricated via Supercritical Fluid-Assisted in Situ Exfoliation ». *ACS Appl Mater Interfaces,* vol. 10, nº 1, p. 1225-1236.

HCN. 2002. *Health Council of the Netherlands Committee on Updating of Occupational Exposure Limits/Methyl ethyl ketone peroxide*.

Hodgkin, J. 2001. « Thermosets: Epoxies and Polyesters ». *Encyclopedia of materials: Science and Technology*.

Holbl. 1995. *Microtome*.

Hong, Seul Ki, Ki Yeong Kim, Taek Yong Kim, Jong Hoon Kim, Seong Wook Park, Joung Ho Kim et Byung Jin Cho. 2012. « Electromagnetic interference shielding effectiveness of monolayer graphene ». *Nanotechnology,* vol. 23, nº 45, p. 455704.

Hontoria-Lucas, C., A. J. López-Peinado, J. de D. López-González, M. L. Rojas-Cervantes et R. M. Martín-Aranda. 1995. « Study of oxygen-containing groups in a series of graphite oxides: Physical and chemical characterization ». *Carbon,* vol. 33, nº 11, p. 1585-1592.

J-P. Pascault, H. Sauterea, J. Verdu. 2002. « Thermosetting Polymers ».

JD Menczel, RB Prime. 2009. *Thermogravimetric Analysis of polymers*.

JMG Cowie, V Arrighi. 2007. *Polymers: chemistry and physics of modern materials*.

Joseph I. Goldstein, Dale E. Newbury, Joseph R. Michael, Nicholas W.M. Ritchie, John Henry J. Scott, David C. Joy. 2017. *Scanning electron microscopy and X-ray microanalysis*.

Kim, Hyunwoo, Ahmed A. Abdala et Christopher W. Macosko. 2010. « Graphene/Polymer Nanocomposites ». *Macromolecules,* vol. 43, nº 16, p. 6515-6530.

Kim, Hyunwoo, Yutaka Miura et Christopher W. Macosko. 2010. « Graphene/Polyurethane Nanocomposites for Improved Gas Barrier and Electrical Conductivity ». *Chemistry of Materials,* vol. 22, nº 11, p. 3441-3450.

Kim, Ju-Young, Kyung-Woo Lee, Jung-Suk Lee et Dongil Kwon. 2006. « Determination of tensile properties by instrumented indentation technique: Representative stress and strain approach ». *Surface and Coatings Technology,* vol. 201, nº 7, p. 4278-4283.

Kowalski, A. J., M. Cooke et S. Hall. 2011. « Expression for turbulent power draw of an in-line Silverson high shear mixer ». *Chemical Engineering Science,* vol. 66, nº 3, p. 241-249.

Kremer, F. 2002. « Dielectric spectroscopy – yesterday, today and tomorrow ». *Journal of Non-Crystalline Solids,* vol. 305, nº 1, p. 1-9.

Kudin K, Scuseria G, Yakobson B. 2001. « Oxygen-driven unzipping graphite materials ». *Phys Rev B*.

Kuilla, Tapas, Sambhu Bhadra, Dahu Yao, Nam Hoon Kim, Saswata Bose et Joong Hee Lee. 2010. « Recent advances in graphene based polymer composites ». *Progress in Polymer Science,* vol. 35, nº 11, p. 1350-1375.

Kuldeep Singh, Anil Ohlan and S.K. Dhwan. 2012. « Polymer-Graphene Nanocomposites: Preparation, Characterization, Properties, and Applications ».

Kumar, Pradip, Uday Narayan Maiti, Kyung Eun Lee et Sang Ouk Kim. 2014. « Rheological properties of graphene oxide liquid crystal ». *Carbon,* vol. 80, p. 453-461.

Kutz, M. 2011. « Applied plastics engineering handbook: processing and materials ». In.

Layek, Rama K., Sanjoy Samanta, Dhruba P. Chatterjee et Arun K. Nandi. 2010. « Physical and mechanical properties of poly(methyl methacrylate) -functionalized graphene/poly(vinylidine fluoride) nanocomposites: Piezoelectric β polymorph formation ». *Polymer,* vol. 51, nº 24, p. 5846-5856.

Lee, Jae-Ung, Duhee Yoon, Hakseong Kim, Sang Wook Lee et Hyeonsik Cheong. 2011. « Thermal conductivity of suspended pristine graphene measured by Raman spectroscopy ». *Physical Review B,* vol. 83, nº 8, p. 081419.

Lee, Seul-Yi;Park, Soo-Jin. 2012. « Comprehensive review on synthesis and adsorption behaviors of graphene-based materials ».

Lian, Yan, Fengjiao He, Huan Wang et Feifei Tong. 2015. « A new aptamer/graphene interdigitated gold electrode piezoelectric sensor for rapid and specific detection of Staphylococcus aureus ». *Biosensors and Bioelectronics,* vol. 65, p. 314-319.

Liang, Jiajie, Yi Huang, Long Zhang, Yan Wang, Yanfeng Ma, Tianyin Guo et Yongsheng Chen. 2009. « Molecular-Level Dispersion of Graphene into Poly(vinyl alcohol) and Effective Reinforcement of their Nanocomposites ». *Advanced Functional Materials,* vol. 19, nº 14, p. 2297-2302.

Liao, Shu-Hang, Min-Chien Hsiao, Chuan-Yu Yen, Chen-Chi M. Ma, Shuo-Jen Lee, Ay Su, Ming-Chi Tsai, Ming-Yu Yen et Po-Lan Liu. 2010. « Novel functionalized carbon nanotubes as cross-links reinforced vinyl ester/nanocomposite bipolar plates for polymer electrolyte membrane fuel cells ». *Journal of Power Sources,* vol. 195, nº 23, p. 7808-7817.

Liu, D., X. Chen, Y. Hu, T. Sun, Z. Song, Y. Zheng, Y. Cao, Z. Cai, M. Cao, L. Peng, Y. Huang, L. Du, W. Yang, G. Chen, D. Wei, A. T. S. Wee et D. Wei. 2018. « Raman enhancement on ultra-clean graphene quantum dots produced by quasi-equilibrium plasma-enhanced chemical vapor deposition ». *Nat Commun,* vol. 9, nº 1, p. 193.

Liu, Qinghong, Xufeng Zhou, Xinyu Fan, Chunyang Zhu, Xiayin Yao et Zhaoping Liu. 2012. « Mechanical and Thermal Properties of Epoxy Resin Nanocomposites Reinforced with Graphene Oxide ». *Polymer-Plastics Technology and Engineering,* vol. 51, nº 3, p. 251-256.

Loos, Marcio. 2015. *Carbon nanotube reinforced composities*.

Lubchenco, Jane. 1998. « Entering the Century of the Environment: A New Social Contract for Science ». *Science,* vol. 279, nº 5350, p. 491.

M.J. Mullins, D. Liu, H.-J.Sue. 2012. « Mechanical properties of thermosets ».

Maddah, Hisham A. 2016. « Polypropylene as a Promising Plastic: A Review ».

McMaster, H.A., Libbey-Owens-For Glass Company, 1947, Conductive Coating for Glass and Method of Application, US Patent 2429420.

Meyer, Gerhard, et Nabil M. Amer. 1988. « Novel optical approach to atomic force microscopy ». *Applied Physics Letters,* vol. 53, nº 12, p. 1045-1047.

Moghimian, Nima, Sajjad Saeidlou, Helen Lentzakis, Gian Flippo Rosi, Naiheng Song et Eric David. 2017. « Electrical conductivity of commercial graphene polyethylene nanocomposites ».

Mohan, Velram Balaji, Reuben Brown, Krishnan Jayaraman et Debes Bhattacharyya. 2015. « Characterisation of reduced graphene oxide: Effects of reduction variables on electrical conductivity ». *Materials Science and Engineering: B,* vol. 193, p. 49-60.

Mohan, Velram Balaji, Krishnan Jayaraman, Manfred Stamm et Debes Bhattacharyya. 2016. « Physical and chemical mechanisms affecting electrical conductivity in reduced graphene oxide films ». *Thin Solid Films,* vol. 616, p. 172-182.

Mohan, Velram Balaji, Kin-tak Lau, David Hui et Debes Bhattacharyya. 2018. « Graphene-based materials and their composites: A review on production, applications and product limitations ». *Composites Part B: Engineering,* vol. 142, p. 200-220.

Morris JE, Iniewski K. 2013. « Graphene, carbon nanotubes, and nanostructures: techniques and applicaitons ».

Novoselov, A. K. Geim and K. S. 2007. « The rise of graphene ». *Natural materials*.

NTP. 1993. *National Toxicology Program/Methyl ethyl ketone peroxide in dimethyl phthalate.*: US.

OBRC. 2013. « The proportion of global use of plastics ».

Ouellette, Robert J., et J. David Rawn. 2015. « 28 - Synthetic Polymers ». In *Organic Chemistry Study Guide*, sous la dir. de Ouellette, Robert J., et J. David Rawn. p. 587-601. Boston: Elsevier.
< http://www.sciencedirect.com/science/article/pii/B9780128018897000285 >.

P.E, Philip A. Schweitzer. 2006. *Corrosion of Polymers and Elastomers*.

Park, Sungjin, et Rodney S. Ruoff. 2009. « Chemical methods for the production of graphenes ». *Nature Nanotechnology,* vol. 4, p. 217.

Pauer, S Taillemite and R. 2009. « Bringt future for vinyl ester resins in corrosion applications ». *Reinf. Plast.*

Pei, S., Q. Wei, K. Huang, H. M. Cheng et W. Ren. 2018. « Green synthesis of graphene oxide by seconds timescale water electrolytic oxidation ». *Nat Commun,* vol. 9, nº 1, p. 145.

Pei, Songfeng, et Hui-Ming Cheng. 2012. « The reduction of graphene oxide ». *Carbon,* vol. 50, nº 9, p. 3210-3228.

Peng, Y., W. Pan, N. Wang, J. E. Lu et S. Chen. 2018. « Ruthenium Ion-Complexed Graphitic Carbon Nitride Nanosheets Supported on Reduced Graphene Oxide as High-Performance Catalysts for Electrochemical Hydrogen Evolution ». *ChemSusChem,* vol. 11, nº 1, p. 130-136.

Perreault, François, Andreia Fonseca de Faria et Menachem Elimelech. 2015. « Environmental applications of graphene-based nanomaterials ». *Chemical Society Reviews,* vol. 44, nº 16, p. 5861-5896.

Petzelt, Jan, Dmitry Nuzhnyy, Viktor Bovtun, Maxim Savinov, Martin Kempa et Ivan Rychetsky. 2013. « Broadband dielectric and conductivity spectroscopy of inhomogeneous and composite conductors ». *physica status solidi (a),* vol. 210, nº 11, p. 2259-2271.

Pissis, P. 2007. *Thermoset nanocomposites for engineering applications*.

Potts, Jeffrey R., Daniel R. Dreyer, Christopher W. Bielawski et Rodney S. Ruoff. 2011. « Graphene-based polymer nanocomposites ». *Polymer,* vol. 52, nº 1, p. 5-25.

Prasher, Ravi. 2010. « Graphene Spreads the Heat ». *Science,* vol. 328, nº 5975, p. 185.

Puckett, Juska and. 1997. « Matrix Resins and Fiber/Matrix Adhesion ». *Composites Engineering Handbook,* vol. 1st ed.

Qin, F., et C. Brosseau. 2012. « A review and analysis of microwave absorption in polymer composites filled with carbonaceous particles ». *Journal of Applied Physics,* vol. 111, nº 6, p. 061301.

Reimer. 2013. *Scanning electron microscopy: physics of image formation and microanalysis*.

Rhoades, Lawrence J. 2008. « The Transformation of Manufacturing in the 21st Century ».

Robertson. 2005. *Food packaging: principles and practice*.

Sabet, Maziyar, Hassan Soleimani et Seyednooroldin Hosseini. 2018. « Effect of addition graphene to ethylene vinyl acetate and low-density polyethylene ». *Journal of Vinyl and Additive Technology,* vol. 24, nº S1, p. E177-E185.

Saleem, Haleema, Anjali Edathil, Thamsanqa Ncube, Jeewan Pokhrel, Sara Khoori, Akhil Abraham et Vikas Mittal. 2016. « Mechanical and Thermal Properties of Thermoset–Graphene Nanocomposites ». *Macromolecular Materials and Engineering,* vol. 301, nº 3, p. 231-259.

Sanchez, Vanesa C., Ashish Jachak, Robert H. Hurt et Agnes B. Kane. 2012. « Biological Interactions of Graphene-Family Nanomaterials: An Interdisciplinary Review ». *Chemical Research in Toxicology,* vol. 25, nº 1, p. 15-34.

Sanjinés, R., M. D. Abad, Cr Vâju, R. Smajda, M. Mionić et A. Magrez. 2011. « Electrical properties and applications of carbon based nanocomposite materials: An overview ». *Surface and Coatings Technology,* vol. 206, nº 4, p. 727-733.

Schuetze, Andrew P., Wayne Lewis, Chris Brown et Wilhelmus J. Geerts. 2004. « A laboratory on the four-point probe technique ». *American Journal of Physics,* vol. 72, nº 2, p. 149-153.

Shahil, Khan M. F., et Alexander A. Balandin. 2012. « Thermal properties of graphene and multilayer graphene: Applications in thermal interface materials ». *Solid State Communications,* vol. 152, nº 15, p. 1331-1340.

Si, Yongchao, et Edward T. Samulski. 2008. « Synthesis of Water Soluble Graphene ». *Nano Letters,* vol. 8, nº 6, p. 1679-1682.

Singh, Virendra, Daeha Joung, Lei Zhai, Soumen Das, Saiful I. Khondaker et Sudipta Seal. 2011. « Graphene based materials: Past, present and future ». *Progress in Materials Science,* vol. 56, nº 8, p. 1178-1271.

Smith, BC. 2011. *Fundamentals of Fourier transform infrared spectroscopy*.

Smits, F. M. 1958. « Measurement of Sheet Resistivities with the Four-Point Probe ». *Bell System Technical Journal,* vol. 37, nº 3, p. 711-718.

Song, Pingan, Zhenhu Cao, Yuanzheng Cai, Liping Zhao, Zhengping Fang et Shenyuan Fu. 2011. « Fabrication of exfoliated graphene-based polypropylene nanocomposites with enhanced mechanical and thermal properties ». *Polymer,* vol. 52, nº 18, p. 4001-4010.

Sreeprasad, T. S., et Vikas Berry. 2013. « How Do the Electrical Properties of Graphene Change with its Functionalization? ». *Small,* vol. 9, nº 3, p. 341-350.

Stankovich, Sasha, Dmitriy A. Dikin, Geoffrey H. B. Dommett, Kevin M. Kohlhaas, Eric J. Zimney, Eric A. Stach, Richard D. Piner, SonBinh T. Nguyen et Rodney S. Ruoff. 2006. « Graphene-based composite materials ». *Nature,* vol. 442, p. 282.

Stannarius, R., F. Kremer et M. Arndt. 1995. « Dynamic Exchange Effects in Broadband Dielectric Spectroscopy ». *Physical Review Letters,* vol. 75, nº 25, p. 4698-4701.

Starr, Ken L. Fordyke and Trevor F. 2002. *Thermoset resin*.

Su, Qi, Shuping Pang, Vajiheh Alijani, Chen Li, Xinliang Feng et Klaus Müllen. 2009. « Composites of Graphene with Large Aromatic Molecules ». *Advanced Materials,* vol. 21, nº 31, p. 3191-3195.

Subbiah Alwarappan, Ashok Kumar. 2013. *Graphene-Based Materials*. Science and Technology.

Suk, Ji Won, Richard D. Piner, Jinho An et Rodney S. Ruoff. 2010. « Mechanical Properties of Monolayer Graphene Oxide ». *ACS Nano,* vol. 4, nº 11, p. 6557-6564.

Sun, Wei, Renzong Hu, Hui Liu, Meiqin Zeng, Lichun Yang, Haihui Wang et Min Zhu. 2014. « Embedding nano-silicon in graphene nanosheets by plasma assisted milling for high capacity anode materials in lithium ion batteries ». *Journal of Power Sources,* vol. 268, p. 610-618.

Taipalus, R., T. Harmia, M. Q. Zhang et K. Friedrich. 2001. « The electrical conductivity of carbon-fibre-reinforced polypropylene/polyaniline complex-blends: experimental characterisation and modelling ». *Composites Science and Technology,* vol. 61, nº 6, p. 801-814.

Tang, Haixiong, Gregory J. Ehlert, Yirong Lin et Henry A. Sodano. 2012a. « Highly Efficient Synthesis of Graphene Nanocomposites ». *Nano Letters,* vol. 12, nº 1, p. 84-90.

Tang, Zhenghai, Hailan Kang, Zuoli Shen, Baochun Guo, Liqun Zhang et Demin Jia. 2012b. « Grafting of Polyester onto Graphene for Electrically and Thermally Conductive Composites ». *Macromolecules,* vol. 45, nº 8, p. 3444-3451.

Teng, Chih-Chun, Chen-Chi M. Ma, Chu-Hua Lu, Shin-Yi Yang, Shie-Heng Lee, Min-Chien Hsiao, Ming-Yu Yen, Kuo-Chan Chiou et Tzong-Ming Lee. 2011. « Thermal conductivity and structure of non-covalent functionalized graphene/epoxy composites ». *Carbon,* vol. 49, nº 15, p. 5107-5116.

Thostenson, Erik T., et Tsu-Wei Chou. 2006. « Processing-structure-multi-functional property relationship in carbon nanotube/epoxy composites ». *Carbon,* vol. 44, nº 14, p. 3022-3029.

Thostenson, Erik T., Saeed Ziaee et Tsu-Wei Chou. 2009. « Processing and electrical properties of carbon nanotube/vinyl ester nanocomposites ». *Composites Science and Technology,* vol. 69, nº 6, p. 801-804.

Utomo, Adi T., Michael Baker et Andrzej W. Pacek. 2008. « Flow pattern, periodicity and energy dissipation in a batch rotor–stator mixer ». *Chemical Engineering Research and Design,* vol. 86, nº 12, p. 1397-1409.

Van Lier, Gregory, Christian Van Alsenoy, Vic Van Doren et Paul Geerlings. 2000. « Ab initio study of the elastic properties of single-walled carbon nanotubes and graphene ». *Chemical Physics Letters,* vol. 326, nº 1, p. 181-185.

van Rooyen, Louis Johann, Jozsef Karger-Kocsis et Lesotlho David Kock. 2015. « Improving the helium gas barrier properties of epoxy coatings through the incorporation of graphene nanoplatelets and the influence of preparation techniques ». *Journal of Applied Polymer Science,* vol. 132, nº 39.

Wang, Guoxiu, Juan Yang, Jinsoo Park, Xinglong Gou, Bei Wang, Hao Liu et Jane Yao. 2008. « Facile Synthesis and Characterization of Graphene Nanosheets ». *The Journal of Physical Chemistry C,* vol. 112, nº 22, p. 8192-8195.

Wang, Jingchao, Xianbao Wang, Chunhui Xu, Min Zhang et Xiaopeng Shang. 2011. « Preparation of graphene/poly(vinyl alcohol) nanocomposites with enhanced mechanical properties and water resistance ». *Polymer International,* vol. 60, nº 5, p. 816-822.

Wang, Shu Jun, Yan Geng, Qingbin Zheng et Jang-Kyo Kim. 2010. « Fabrication of highly conducting and transparent graphene films ». *Carbon,* vol. 48, nº 6, p. 1815-1823.

Williams, Tim, 2017, Chapter 15 - Shielding, EMC for Product Designers (Fifth Edition), p.435-456.

Worsley, Marcus A., Peter J. Pauzauskie, Tammy Y. Olson, Juergen Biener, Joe H. Satcher et Theodore F. Baumann. 2010. « Synthesis of Graphene Aerogel with High Electrical Conductivity ». *Journal of the American Chemical Society,* vol. 132, nº 40, p. 14067-14069.

Wu, Chao, Xingyi Huang, Genlin Wang, Libing Lv, Gan Chen, Guangyv Li et Pingkai Jiang. 2013. « Highly Conductive Nanocomposites with Three-Dimensional, Compactly Interconnected Graphene Networks via a Self-Assembly Process ». *Advanced Functional Materials,* vol. 23, nº 4, p. 506-513.

Wu, Hang, Weifeng Zhao et Guohua Chen. 2012. « One-pot in situ ball milling preparation of polymer/graphene nanocomposites ». *Journal of Applied Polymer Science,* vol. 125, nº 5, p. 3899-3903.

Xie, Q., M. A. Alibakhshi, S. Jiao, Z. Xu, M. Hempel, J. Kong, H. G. Park et C. Duan. 2018. « Fast water transport in graphene nanofluidic channels ». *Nat Nanotechnol*.

Yang, Wenrong, Kyle R. Ratinac, Simon P. Ringer, Pall Thordarson, J. Justin Gooding et Filip Braet. 2010. « Carbon Nanomaterials in Biosensors: Should You Use Nanotubes or Graphene? ». *Angewandte Chemie International Edition,* vol. 49, nº 12, p. 2114-2138.

Yu, J., X. Huang, C. Wu et P. Jiang. 2011. « Permittivity, thermal conductivity and thermal stability of poly(vinylidene fluoride)/graphene nanocomposites ». *IEEE Transactions on Dielectrics and Electrical Insulation,* vol. 18, nº 2, p. 478-484.

Z, Liu. 2015. *Graphene: energy storage and conversion applications*.

Zhang, Hao-Bin, Wen-Ge Zheng, Qing Yan, Yong Yang, Ji-Wen Wang, Zhao-Hui Lu, Guo-Ying Ji et Zhong-Zhen Yu. 2010. « Electrically conductive polyethylene terephthalate/graphene nanocomposites prepared by melt compounding ». *Polymer,* vol. 51, nº 5, p. 1191-1196.

Zhang, Jinli, Shuangqing Xu et Wei Li. 2012. « High shear mixers: A review of typical applications and studies on power draw, flow pattern, energy dissipation and transfer properties ». *Chemical Engineering and Processing: Process Intensification,* vol. 57-58, p. 25-41.

Zhang, Li Li, Xin Zhao, Meryl D. Stoller, Yanwu Zhu, Hengxing Ji, Shanthi Murali, Yaping Wu, Stephen Perales, Brandon Clevenger et Rodney S. Ruoff. 2012. « Highly Conductive and Porous Activated Reduced Graphene Oxide Films for High-Power Supercapacitors ». *Nano Letters,* vol. 12, nº 4, p. 1806-1812.

Zhang, Xi, Vahid Bitaraf, Suying Wei, Zhanhu Guo, Xi Zhang, Suying Wei et Henry A. Colorado. 2014. « Vinyl ester resin: Rheological behaviors, curing kinetics, thermomechanical, and tensile properties ». *AIChE Journal,* vol. 60, nº 1, p. 266-274.

Zhang, Z. L., M. Hauge, J. Ødegård et C. Thaulow. 1999. « Determining material true stress–strain curve from tensile specimens with rectangular cross-section ». *International Journal of Solids and Structures,* vol. 36, nº 23, p. 3497-3516.

Zhanhu Guo, Tony Pereira, Oyoung Choi, Ying Wang, H. Thomas Hahn. 2006. « Surface functionalized alumina nanoparticle filled polymeric nanocomposites with enhanced mechanical properties ».

Zhao, B., C. Zhao, R. Li, S. M. Hamidinejad et C. B. Park. 2017a. « Flexible, Ultrathin, and High-Efficiency Electromagnetic Shielding Properties of Poly(Vinylidene Fluoride)/Carbon Composite Films ». *ACS Appl Mater Interfaces,* vol. 9, nº 24, p. 20873-20884.

Zhao, Biao, Chongxiang Zhao, Ruosong Li, S. Mahdi Hamidinejad et Chul B. Park. 2017b. « Flexible, Ultrathin, and High-Efficiency Electromagnetic Shielding Properties of Poly(Vinylidene Fluoride)/Carbon Composite Films ». *ACS Applied Materials & Interfaces,* vol. 9, nº 24, p. 20873-20884.

Zhu, Yanwu, Shanthi Murali, Weiwei Cai, Xuesong Li, Ji Won Suk, Jeffrey R. Potts et Rodney S. Ruoff. 2010. « Graphene and Graphene Oxide: Synthesis, Properties, and Applications ». *Advanced Materials,* vol. 22, nº 35, p. 3906-3924.